

This document includes:

1. Revision (text and table and figures)
2. Comment and response
3. Annotated revision

1 **A non-stationary earthquake probability assessment with Mohr-Coulomb failure**
2 **criterion: including an application to central Taiwan**

3
4 **Abstract:** From theory to experience, earthquake probability associated with an active
5 fault should be gradually increasing with time since the last event. In other words, the
6 process should be non-stationary, rather than being stationary as the Poisson process. In
7 this paper, a new non-stationary earthquake assessment is introduced. Different from
8 other analyses, the new model more clearly defines and calculates two stress states or
9 boundary conditions between two consecutive earthquakes, facilitated with the Mohr-
10 Coulomb failure criterion. In addition to the model development, this paper also presents
11 a model application to evaluate earthquake probability associated with the Meishan fault
12 in central Taiwan. Based on the best-estimate return period of 162 ± 50 years, focal
13 depth of 4 ~ 8 km, etc., there could be a 7.6% probability for the fault to induce a major
14 earthquake in years 2015 ~ 2025, and if the earthquake does not recur by 2025, the
15 earthquake probability will increase to 8% in 2025 ~ 2035, a non-stationary probability
16 depending on the starting dates of a given period of time.

17
18 **Keyword:** non-stationary earthquake probability assessment, Mohr-Coulomb failure
19 criterion

20
21 J.P. Wang; Dept Civil & Environmental Engineering, Hong Kong University of Science and
22 Technology, Kowloon, Hong Kong

23 Yun Xu; Dept Civil & Environmental Engineering, Hong Kong University of Science and
24 Technology, Kowloon, Hong Kong

24 **1. Introduction**

25 Owing to our imperfect understandings and natural randomness of earthquake,
26 several models have been proposed for estimating earthquake probability in a given
27 period of time. Among them, the Poisson model might be the one that is mostly used in
28 many applications (e.g., Weichert, 1980; Ang and Tang, 2007; Ashtari Jafari, 2010).
29 However, it must be noted that the Poisson calculation is a “memory-less” model (Devore,
30 2008), meaning that the Poissonian probability is only a function of length of time, but
31 irreverent to when the last earthquake was occurring.

32 However, it seems that the recurrence of a characteristic earthquake associated
33 with a given active fault should not be stationary or memory-less. That is, the earthquake
34 probability should be gradually increasing with time. Taking the recent Nepal earthquake
35 in April 2015 for example, the probability for the very next Nepal earthquake to recur in
36 2015 ~ 2020 should be lower than that in 2115 ~ 2120, although the two have the same
37 length of time.

38 The scope of this study is to develop a new non-stationary earthquake probability
39 assessment, mainly from the concepts of the Mohr-Coulomb failure criterion. Meanwhile,
40 this paper provides a comprehensive review on other non-stationary earthquake models
41 (Section Two), followed by our non-stationary analysis (Section Three). Then, the new
42 model is demonstrated with a model application to central Taiwan (Section Four), as well
43 as model improvement and future work (Section Five).

44

45 **2. An overview of non-stationary earthquake models**

46 In this section, we would like to provide a comprehensive review on non-
47 stationary earthquake analyses and models. Specifically, we characterized the models
48 into two groups, referred to as “statistical models” and “physical model.”

49

50 2.1 Statistical models

51 Basically, those statistical models developed are more or less a derivative of the
52 stationary Poisson model. For example, Vere-Jones and Ozaki (1982) proposed the use
53 of a time-variant model parameter for the Poissonian calculation, making their model
54 non-stationary although the calculation is still Poissonian in essence. Similarly, another
55 work suggested the use of adjusted return period (related to current time and original
56 return period) for the Poissonian calculation, in order to modify the Poisson model from
57 stationary to non-stationary (Wang et al., 2013).

58 Another type of modification is to use non-exponential distributions to model
59 earthquake inter-occurrence time intervals as a random variable. (Note that for an event
60 modeled by a Poisson process, the number of events in a given period of time is a discrete
61 random variable following the Poisson distribution; meanwhile the time when the next
62 event would recur is a continuous variable following the exponential distribution.) For
63 example, the log-normal distribution (Ferrães, 2005), Weibull distribution (Yakovlev et
64 al., 2006), and Gamma distribution (Gómez and Pacheco, 2004) have been suggested for
65 the replacement of the exponential distribution, with them all featuring a non-stationary
66 analysis after such modifications.

67 Based on given earthquake data, it must be noted that the statistical models are all
68 empirical in a sense. In other words, the models are in no consideration of earthquake
69 mechanisms, such as tectonic stress accumulation under the ground.

70

71 2.2 Physical models

72 In consideration of earthquake mechanics, several non-stationary earthquake
73 analyses have also been proposed from a different perspective. It must be noted that the
74 models are not entirely a “product” of physics, but somehow on the basis of the concepts
75 of physics working together with empirical models. Specifically, we would like to
76 introduce three of them in the following that are more related to our non-stationary
77 earthquake model.

78 The first one we like to introduce here is the time-predictable model (Shimazaki
79 and Nakata, 1980). Fig. 1 is a schematic diagram illustrating the model basics.
80 Essentially, the model is relying on a best-estimate relationship between co-seismic fault
81 slip (or displacement) and time. For instance, given the last event with fault slips as
82 Points A and B (see Fig. 1), then the next event should recur at the time of Points C and
83 D. In other words, the recent event with a smaller fault slip should accompany a smaller
84 stress drop, and under a constant stress increment with time, it should lead to a shorter
85 time for the stress to re-reach a stress level (or failure stress state) that could induce
86 earthquakes.

87 The next model of the group is the Brownian model (Ellsworth et al., 1999;
88 Matthews et al., 2002). By contrast to the time-predictable model, the Brownian model is
89 not on the basis of a constant stress increment, while considering the stress increments

90 between two consecutive events should be a stochastic process like Fig. 2. Specifically,
91 the model considers the stress-time series is a combination of a long-term stress
92 increment and a Brownian motion simulating transient stress randomness. With such a
93 function, we can estimate the time of the next earthquake by examining if the stress
94 reaches the failure state within a given period of time.

95 The third one we like to introduce is the negative binomial model (Tejedor et al.,
96 2015). As the previous analyses, the model is also on the basis of two imaginary stress
97 states. As shown in Fig. 3, the essence of the model is that the stress change in unit time
98 could be modeled by two scenarios: stress does and does not increase. As a result, there
99 are many possible “stress routes” (as shown in Fig. 3) between two consecutive events,
100 and the probability and the total time of each route could be calculated with given
101 earthquake return periods. Finally, the inter-occurrence time interval can be derived as a
102 negative binomial distribution for such a non-stationary probability assessment.

103 To sum up, the three physical models are all facilitated with two stress states that
104 are part of the earthquake occurrence theories generally accepted. Somehow, we do
105 share this perspective for our model development. However, the biggest difference is
106 that our model defines and calculates the two stress states more clearly, on the basis of
107 the Mohr-Coulomb failure criterion that is well established and used in rock mechanics,
108 structural geology, etc.

109

110 **3. The new non-stationary earthquake probability assessment**

111 3.1 Overviews of Mohr-Coulomb failure criterion and elastic rebound theory

112 The Mohr-Coulomb failure criterion is a model describing the response of
113 materials subject to external stresses (Pariseau, 2007), and it is commonly applied to rock
114 mechanics as well as other applications. Fig. 4 is a schematic diagram illustrating the
115 essentials of the model. Basically, as the Mohr circle is below the failure envelope, a
116 shear failure is not expected in the material. By contrast, as long as the Mohr circle is in
117 contact with the failure envelope, a shear failure could occur.

118 On the other hand, it is generally accepted that the ongoing tectonic activities are
119 the main reason causing rock failures under the ground, resulting in an earthquake with
120 the release of accumulated strain energy. Afterward, the energy re-accumulates and re-
121 releases until the next earthquake, and such a theory is referred to as the elastic rebound
122 theory (Keller, 1996), proposed by Reid in the early twentieth century (Reid, 1910).

123

124 3.2 The model basics and the algorithms

125 The two earthquake theories above were mainly the motivation of the new non-
126 stationary model: 1) based on the Mohr-Coulomb failure criterion, the rock subject to the
127 stress state as Mohr Circle C (see Fig. 4) should fail and cause an earthquake, at which
128 we refer to it as failure state; 2) from the elastic rebound theory, the stress state in the
129 rock right after a characteristic earthquake should be restored to Mohr Circle A, which is
130 called the initial state at time t_0 .

131 As a result, the problem to evaluate the earthquake probability within a given time
132 t^* after the last event (or after t_0) is becoming a problem as follows: What is the chance
133 for the major principle stress at time t^* (denoted as $\sigma_{1_{t^*}}$) greater than the major principle

134 stress at the failure state (denoted as $\sigma_{1_failure}$)? Or the question can be mathematically
135 expressed by the following equation:

136

$$137 \Pr(\text{earthquake within } t^* \text{ after } t_0) = \Pr(\sigma_{1_t^*} > \sigma_{1_failure}) \quad (1)$$

138

139 Clearly, the problem now is governed by two variables $\sigma_{1_t^*}$ and $\sigma_{1_failure}$, and their
140 relationships with other parameters will be detailed later. Note that those notations used
141 in the following derivations are summarized in the end of the paper.

142

- 143 • The major principle stress at failure state, $\sigma_{1_failure}$

144 Based on the Mohr-Coulomb failure criterion, the major principal stress at failure
145 state (Point C in Fig. 4) can be expressed as a function of the minor principal stress at
146 failure ($\sigma_{3_failure}$), and two strength parameters of the shearing plane, i.e., cohesion c and
147 friction angle ϕ (Pariseau, 2007):

148

$$149 \sigma_{1_failure} = \sigma_{3_failure} \left(\frac{1 + \sin \phi}{1 - \sin \phi} \right) + \frac{2c \times \cos \phi}{1 - \sin \phi} \quad (2)$$

150

- 151 • The minor principal stress at failure state, $\sigma_{3_failure}$

152 The minor principal stress at failure is attributed to the overburden earth pressure
153 above the focal depth d , which can be estimated with the following formula based on
154 rock mechanics:

155

156
$$\sigma_{3_failure} = \gamma \times d \tag{3}$$

157

158 where γ is rock unit weight. It must be noted that this model considers $\sigma_{3_failure}$ as time-
159 invariant (more discussion is given later), and the case shown in Fig. 4 and Eq. 3 is for a
160 thrust-fault earthquake. As for the strike-slip fault, the Mohr circles of the initial state
161 and the failure state are shown in Fig. 5, indicating $\sigma_{3_failure}$ is equal to $\gamma \times d \times K$ for this
162 case, where K is the coefficient of lateral earth pressure in rock. More discussion over
163 model improvements is given in Section 5.2.

164

- 165 • The major principle stress at time t^* , $\sigma_{1_t^*}$

166 With tectonic stress increasing with time, the key task of the new analysis is to
167 estimate the major principle stress at time t^* after the last event. For thrust-fault
168 earthquakes as those Mohr circles shown in Fig. 4, the major principle stress at time t^*
169 can be formulated as follows:

170

171
$$\sigma_{1_t^*} = \sigma_{3_initial} + t^* \times ASI \tag{4}$$

172

173 where $\sigma_{3_initial}$ is the minor principal stress at the initial state (or at t_0) and ASI is called
174 annual stress increment. Note that from Fig. 4 (the thrust fault) and Fig. 5 (the strike-slip
175 fault), $\sigma_{3_initial}$ is equal to $\gamma \times d \times K$ for the two cases of the non-stationary analysis.

176

177 3.3 The return period \tilde{t} and its relationship with $\sigma_{1_{t^*}}$

178 In addition to γ, d, K , etc., the return period \tilde{t} of characteristic earthquakes is
179 another input data of the non-stationary analysis. Moreover, the mean value and standard
180 deviation of $\sigma_{1_{t^*}}$ can be expressed as a function of \tilde{t} , and used for developing its
181 probability density function for the non-stationary probability assessment within the
182 given time t^* .

183 From the meaning of return period, it is understood that the event will recur when
184 return period \tilde{t} is due. As a result, the major principal stress at return period \tilde{t} (denoted
185 as $\sigma_{1_{\tilde{t}}}$) should be equal to $\sigma_{1_{failure}}$:

186

187
$$\sigma_{1_{\tilde{t}}} = \sigma_{3_{initial}} + \tilde{t} \times ASI = \sigma_{1_{failure}} \quad (5)$$

188

189 Therefore, the mean value of ASI (denoted as μ_{ASI}) can be derived as follows:

190

191
$$E[\sigma_{1_{failure}}] = E[\sigma_{3_{initial}} + \tilde{t} \times ASI] \quad (6)$$

$$\Rightarrow E[ASI] = \frac{\sigma_{1_{failure}} - \sigma_{3_{initial}}}{\tilde{t}} = \mu_{ASI}$$

192

193 where $E[]$ denotes the mean value of a variable in probability and statistics.

194 On the other hand, as the variability of annual stress increment is equal to n in
195 terms of coefficient of variation (= standard deviation / mean value), its standard
196 deviation (denoted as s_{ASI}) can be derived as follows with its mean value from Eq. 6:

197

$$198 \quad n = \frac{s_{ASI}}{\mu_{ASI}} \Rightarrow s_{ASI} = n \times \mu_{ASI} = \frac{n \times (\sigma_{1_failure} - \sigma_{3_initial})}{\tilde{t}} \quad (7)$$

199

200 With the mean (Eq. 6) of ASI , we can continue deriving the mean value of the major

201 principal stress at time t^* :

202

$$\sigma_{1_t^*} = \sigma_{3_initial} + t^* \times ASI$$

$$203 \quad \Rightarrow E[\sigma_{1_t^*}] = E[\sigma_{3_initial} + t^* \times ASI] = \sigma_{3_initial} + t^* \times E[ASI] \quad (8)$$

$$= \sigma_{3_initial} + \frac{t^* \times (\sigma_{1_failure} - \sigma_{3_initial})}{\tilde{t}}$$

204

205 Similarly, the standard deviation of the major principal stress at time t^* (denoted as $s_{\sigma_{1_t^*}}$)

206 can be derived as follows with s_{ASI} in Eq. 7:

207

$$\sigma_{1_t^*} = \sigma_{3_initial} + t^* \times ASI$$

$$208 \quad \Rightarrow V[\sigma_{1_t^*}] = V[\sigma_{3_initial} + t^* \times ASI] = t^{*2} \times V[ASI] = t^{*2} \times s_{ASI}^2 \quad (9)$$

$$\Rightarrow s_{\sigma_{1_t^*}} = \sqrt{V[\sigma_{1_t^*}]} = t^* \times s_{ASI} = \frac{t^* \times n \times (\sigma_{1_failure} - \sigma_{3_initial})}{\tilde{t}}$$

209

210 where $V[\]$ denotes variance in probability and statistics, and it is the square of standard

211 deviation.

212 In order to establish the probability density function of σ_{1-t^*} , the information
213 about what probability distribution the variable is following is as essential as its mean
214 value and standard deviation. But since the distribution of σ_{1-t^*} is unknown (to the best
215 of our knowledge, no study has ever worked on the subject), we suggest the normal
216 distribution for this non-stationary earthquake assessment, as it is usually recommended
217 for a probability analysis when the variables' distribution is unknown (Abramson et al.,
218 2002).

219

220 3.4 Summary

221 Fig. 6 is a schematic diagram illustrating the essentials of the non-stationary
222 assessments. The key to the model is to estimate the probability distribution of the major
223 principal stress at time t^* after the last event (or after t_0), and compares it to the stress that
224 could cause rock failures and earthquakes. To sum up, the new non-stationary model is
225 governed by a total of six parameters as follows: return period (\tilde{t}), fault-plane strength
226 parameters (c and ϕ), rock unit weight (γ), earthquake focal depth (d), and the
227 variability of annual stress increment in terms of coefficient of variation (n).

228

229 3.5 Presumption and limitation

230 The elastic rebound theory is a plausible explanation to earthquake, but
231 specifically speaking, it is more of a theory about main shocks. As a result, the new non-
232 stationary analysis of the study motivated by such a theory is more applicable to main
233 shocks, a situation similar to other non-stationary models that are also applicable to main

234 shocks rather than dependent shocks (Shimazaki and Nakata, 1980; Ellsworth, 1995;
235 Matthews et al., 2002; Tejedor et al., 2015).

236 On the other hand, like any other stationary or non-stationary analyses estimating
237 earthquake probability in a given period of time, our model cannot predict the magnitude
238 of the recurring event, either. In other words, the (earthquake) temporal analyses closely
239 related to return period, stress increment, etc. do not further relate the variables to
240 earthquake magnitudes or energy release. Again, such a framework is similar to other
241 stationary or non-stationary temporal analyses only focusing on the earthquake
242 probability in a given period of time, but not on the probability distribution of earthquake
243 magnitude or energy release when the event recurs.

244

245 **4. A model application**

246 **4.1 The Meishan earthquake in central Taiwan**

247 The region around Taiwan is known for high seismicity owing to the location
248 close to the boundaries of tectonic plates. On average, there are around 2,000
249 earthquakes above M_w 3.0 (moment magnitude) occurring around Taiwan every year,
250 with a catastrophic event, like the M_w 6.4 Meishan earthquake in 1906 and the M_w 7.6
251 Chi-Chi earthquake in 1999, that could recur in decades.

252 As a result, we would like to apply the new non-stationary model to Taiwan as a
253 case study. Specifically, we selected the Meishan fault in central Taiwan as the model
254 application, given a few recent studies pointing out the fault should be of “imminent”
255 earthquake risk, for the event’s return period being “almost” due (e.g., Wang et al., 2012).
256 By contrast, the reason we did not select the Chelungpu fault as the application is because

257 the active fault should be of lower earthquake risk in next couple decades, given it “just”
258 induced the Chi-Chi earthquake in 1999, and should have a longer return period (about
259 250 years) than the Meishan earthquake (Cheng et al., 2007). More discussion over this
260 model application is given in Section 5.1.

261 Fig. 7 shows the location of the Meishan fault in central Taiwan. Accordingly,
262 the fault is very close to a major city (i.e., Chiayi) in central Taiwan, and reportedly the
263 1906 Meishan earthquake killed around 1,200 people in the area.

264

265 4.2 The best-estimate data from the literature

266 Table 1 summarizes our best-estimate data from the literature for the non-
267 stationary earthquake assessment on the Meishan fault. It must be noted that because the
268 strength parameters of the fault plane are not clear, we used a typical range (see Table 1)
269 from rock mechanics as our best estimates. Similarly, a probable range of 0.2 ~ 0.5 was
270 used as our best estimate for the coefficient of lateral earth pressure in rock, given no
271 site-specific studies and data have been reported. As for the earthquake focal depth, we
272 considered the depth should be close to 6 km as the last Meishan earthquake (Ng et al.,
273 2009). However, in order to account for the focal-depth uncertainty in the analysis, we
274 used a best-estimate range as 4 ~ 8 km.

275 A similar situation was encountered in the determination of the best-estimate
276 return period. On the basis of 162 years used in recent studies (e.g., Wang et al., 2012),
277 two best-estimate ranges were determined as 162 ± 50 years and 162 ± 100 years.
278 Understandably, the uncertainties (i.e., ± 50 and ± 100) are from our best judgments,
279 given such information is not clear from the literature. As for the variability of annual

280 stress increment, to the best of our knowledge, there is no any research so far that can
281 really answer the question. As a result, the range of 0.25 ~ 1 was used as our best
282 estimate characterizing the variability of annual stress increment in terms of coefficient of
283 variation.

284 More discussion about the input data characterizations and the model application
285 is given in Section 5.1 in the following.

286

287 4.3 Monte Carlo Simulation

288 Because our input data were characterized by a range rather than a single value, it
289 is difficult to solve the governing equation (Eq. 1) of the non-stationary probability with
290 analytical approaches. Therefore, we used Monte Carlo Simulation (MCS) to solve the
291 problem as many MCS applications. For more details about Monte Carlo Simulation,
292 readers can refer to the textbooks of Ang and Tang (2007), Abramson et al. (2002),
293 among many others.

294

295 4.4 The result

296 With the best-estimate input data summarized in Table 1, Fig. 8 shows the
297 average probabilities for three 10-year periods from Monte Carlo Simulation with a
298 sample size of 5,000. For example, the non-stationary model shows a 7.6% probability
299 for the Meishan fault in central Taiwan to induce a major earthquake in years 2015 ~
300 2025, under the return period of 162 ± 50 years. Then, if the event does not recur by
301 2025, the earthquake probability in 2025 ~ 2035 will increase to 8%; similarly, if the
302 event does not recur by 2035, the probability will further increase to 8.4%. Note that the

303 standard deviations of the three probability estimates are all close to 3.3%, which is a
304 reflection to the input data that were characterized by a range. In other words, if the input
305 data were all characterized by single values, the standard deviation of the probability
306 estimates cannot be calculated and reported.

307 In addition, the Poissonian probabilities for the same problem are also shown in
308 Fig. 8. It shows that for a 10-year period of time, the earthquake probability is about 6%
309 for the three different periods (i.e., 2015 ~ 2025, 2025 ~ 2035, and 2035 ~ 2045), or the
310 probability is irrelevant to the starting dates of the time period.

311 Fig. 9 shows the result for the other scenario under return period as 162 ± 100
312 years. Interestingly, the average probabilities for the three 10-year periods become
313 relatively close to one another, and they are smaller than those estimates subject to the
314 return period of 162 ± 50 years. Our explanation to this is as follows: As shown in Fig.
315 10, the relationship between return period and earthquake probability could be highly
316 non-linear. Therefore, the average probability subject to a bigger range of return period
317 would be lower than that subject to a smaller range. Nevertheless, with the non-
318 stationary model, the probability estimates do vary with the starting dates of the time, or
319 the probabilities are indeed non-stationary, in contrast to the stationary Poisson process.

320

321 **5. Discussions**

322 5.1 Input data characterizations

323 As many analyses, input data characterizations are equally challenging as the
324 model development. As a result, for improving the model estimates, we hope to see more
325 studies focusing on site characterizations with more laboratory works or field

326 instrumentation assessing stress increment variability, fault-plane strength parameters,
327 lateral earth pressure in rock, etc. However, this is beyond the scope of the study
328 focusing on a new non-stationary model development.

329 On the other hand, one could argue why not choose a geologically well-
330 investigated fault (e.g., the Chelungpu fault) in Taiwan as the model application to reduce
331 uncertainty, and here is our response: The “rock-mechanics” parameters of the model
332 (such as lateral pressure coefficients, variability of stress increment, and the strength
333 parameters of fault planes) are not clear either, even for those so-called well-investigated
334 faults in Taiwan. As a result, no matter which fault was selected as the model application,
335 engineering judgment must involve in the determinations of those “rock-mechanics”
336 parameters, more or less creating the same level of uncertainty when it comes to site
337 characterizations on stress increment variability, lateral earth pressure in rock, etc.

338 Besides, as mentioned previously the key reason of using the Meishan fault as a
339 case study is owing to its imminent earthquake risk, not to mention the well-characterized
340 return period of 162 years from the Central Geological Survey Taiwan (Lin et al., 2008)
341 could somewhat help increase the reliability of the estimate, in a comparison to other
342 cases without a well-characterized earthquake return period, or at least not yet reported.

343

344 5.2 Model improvements

345 Certainly, the non-stationary analysis of the study can be further modified. For
346 example, in addition to the algorithms for thrust faults and strike-slip faults that have
347 been derived, the model is also applicable to normal faults as those Mohr circles shown in
348 Fig. 11. Accordingly, the minor principal stress at initial state ($\sigma_{3_initial}$) is equal to

349 $\gamma \times d \times K$ for this case, with the minor principal stress at time t^* (denoted as $\sigma_{3_{t^*}}$) that
350 can be expressed as $\sigma_{3_{initial}} - t^* \times ASI$. Next, the same probability calculation is
351 applicable by comparing the minor principal stress at t^* to the minor principal stress at
352 failure ($\sigma_{3_{failure}}$), for such a normal-fault earthquake subject to tectonic extension.

353 Further improvements can be conducted with the consideration of the direction of
354 stress increment, or the direction of tectonic compression/extension. Under the
355 circumstances, the Mohr circles of the initial state and failure state are shown in Fig. 12,
356 with major and minor principal stresses both varying with time.

357 Nevertheless, no matter how the non-stationary model will evolve, such type of
358 non-stationary analysis from the Mohr-Coulomb failure criterion is as novel, robust and
359 transparent as its counterparts, providing a new alternative to non-stationary earthquake
360 assessment related to a given active fault.

361

362 5.3. Earthquake should be stationary or non-stationary?

363 Although characteristic earthquakes related to a given active fault should be non-
364 stationary, in the 1970s a study has provided statistical evidence to the opposite:
365 earthquake is stationary (Gardner and Knopoff, 1974). However, it must be noted that
366 the study was not focusing on characteristic earthquakes, but based on the regional
367 seismicity in California.

368 Fig. 13 is a schematic diagram that helps explain the difference between the two
369 problems. For each fault, the recurring earthquake should be a non-stationary process,
370 and the non-stationary earthquake probability would be reset at the last event and
371 gradually increase with time. By contrast, the seismicity in a region would become

372 stationary with so many non-stationary processes present. For example, at $T = t_0$ (see Fig.
373 13), the sum of that many stationary probabilities should be close to that at $T = t_1$ (or at
374 any moment), although the earthquake probability induced by Fault D should be very low
375 at $T = t_0$, while others are higher.

376 The relationship can be simply explained with the patron-and-bank analogy. For
377 each patron (analogy to each fault), going to the bank is obviously a non-stationary
378 process, with the probability increasing with time since the very last visit. But for the
379 banks (analogy to the seismicity), it is a stationary process for them, as dealing with so
380 many patrons or so many non-stationary processes at one time.

381

382 **6. Summary and conclusion**

383 Given the earthquake recurrence associated with an active fault that should be a
384 non-stationary process, this paper introduces a new non-stationary analysis to evaluate
385 earthquake probability within a given period of time. Different from previous models,
386 the new analysis more clearly defines and calculates two earthquake stress states, on the
387 basis of the well-established, Mohr-Coulomb failure criterion.

388 In addition, this paper also presents a model application to evaluate earthquake
389 probability associated with the Meishan fault in central Taiwan. With the best-estimate
390 return period of 162 ± 50 years, focal depth of 4 ~ 8 km, etc., the active fault has a 7.6%
391 probability (standard deviation equal to 3.3%) of inducing the next Meishan earthquake
392 in 2015 ~ 2025, and if the earthquake does not recur by 2025, then the non-stationary
393 probability will increase to 8% in 2025 ~ 2035, rather than being unchanged, stationary,
394 or independent of the starting dates of a given period of time.

395 **Notations**

t_0	The time when the last event occurs
t^*	The time interval after the last event
$\sigma_{1_{t^*}}$	Major principle stress at time t^*
$\sigma_{1_{failure}}$	Major principle stress at failure state
$\sigma_{3_{failure}}$	Minor principal stress at failure state
c	Cohesion of the fault plane
ϕ	Friction angle of the fault plane
d	Earthquake focal depth
γ	Rock unit weight
K	Coefficient of lateral earth pressure in rock
ASI	Annual stress increment
\tilde{t}	Earthquake return period
$\sigma_{1_{\tilde{t}}}$	Major principal stress at return period
E	Expected value or mean value
V	Variance
μ_{ASI}	Mean value of ASI
n	Coefficient of variation for ASI
s_{ASI}	Standard deviation of ASI
$s_{\sigma_{1_{t^*}}}$	Standard deviation of $\sigma_{1_{t^*}}$
$\sigma_{1_{initial}}$	Major principal stress at initial state
$\sigma_{3_{initial}}$	Minor principal stress at initial state
$\sigma_{3_{t^*}}$	Minor principal stress at t^*

396

397 **Acknowledgements**

398 We appreciate the comments on the submission from Editor Dr. Malamud,
399 reviewer Dr. Chan of Nanyang Technological University and the anonymous reviewer,
400 making it much improved in so many aspects after revision. We also appreciate the

401 financial support on the research from the Hong Kong University of Science and
402 Technology (Grant: FSECS13EG01).

403

404 **References**

405 Abramson, L. W., Lee, T. S., Sharma, S., and Boyce, G. M.: Slope Stability and
406 Stabilization Methods, John Wiley & Sons, Inc., NJ, 2002.

407 Ang, A. H. S., and Tang, W. H.: Probability Concepts in Engineering: Emphasis on
408 Applications to Civil and Environmental Engineering, 2nd Edn., John Wiley & Sons,
409 Inc., NJ, 2007.

410 Ashtari Jafari, M.: Statistical prediction of the next great earthquake around Tehran, J.
411 Geodyn., 49, 14-18, 2010.

412 Cheng, C. T., Chiou, S. J., Lee, C. T., and Tsai, Y. B.: Study on probabilistic seismic
413 hazard maps of Taiwan after Chi-Chi earthquake, J. GeoEng., 2, 19-28, 2007.

414 Devore, J. L.: Probability and Statistics for Engineering and the Sciences, Brooks/Cole,
415 Boston, Massachusetts, 2008.

416 Ellsworth, W. L., Matthews, M. V., Nadeau, R. M., Nishenko, S. P., Reasenber, P. A.,
417 and Simpson, R. W.: A physically based earthquake recurrence model for estimation
418 of long-term earthquake probabilities, US Department of the Interior, US Geological
419 Survey, 1999.

420 Ferráes, S. G.: A probabilistic prediction of the next strong earthquake in the Acapulco-
421 San Marcos segment, Mexico, Geofisica internacional, 44, 347-353, 2005.

422 Gardner, J. K., and Knopoff, L.: Is the sequence of earthquakes in southern California,
423 with aftershocks removed, Poissonian? Bull. Seismol. Soc. Am., 64, 1363-1367, 1974.

424 Gómez, J. B., and Pacheco, A. F.: The minimalist model of characteristic earthquakes as
425 a useful tool for description of the recurrence of large earthquakes, *Bull. Seismol. Soc.*
426 *Am.*, 94, 1960-1967, 2004.

427 Keller, E. A.: *Environmental Geology*, 7th Edn., Prentice Hall, Inc., NJ, 1996.

428 Lin, C. W., Lu, S. T., Shih, T. S., Lin, W. H., Liu, Y. C., and Chen, P. T.: Active faults of
429 central Taiwan, Special Publication of Central Geological Survey 21,148 (In Chinese
430 with English Abstract), 2008.

431 Matthews, M. V., Ellsworth, W. L., and Reasenber, P. A.: A Brownian model for
432 recurrent earthquakes, *Bull. Seismol. Soc. Am.*, 92, 2233-2250, 2002.

433 Ng, S. M., Angelier, J., and Chang, C. P.: Earthquake cycle in Western Taiwan: Insights
434 from historical seismicity, *Geophys. J. Int.*, 178, 753-774, 2009.

435 Pariseau, W. G.: *Design Analysis in Rock Mechanics*, Taylor & Francis/Balkema, 2007.

436 Reid, H. F.: The mechanics of the earthquake, the California Earthquake of April 18,
437 1906, Report of the State Investigation Commission, Carnegie Institution of
438 Washington, Washington, D.C., 2, 1910.

439 Shimazaki, K., and Nakata, T.: Time-predictable recurrence model for large earthquakes,
440 *Geophys. Res. Lett.*, 7, 279-282, 1980.

441 Tejedor, A., Gómez, J. B., and Pacheco, A. F.: The negative binomial distribution as a
442 renewal model for the recurrence of large earthquakes, *Pure Appl. Geophys.*, 172, 23-
443 32, 2015.

444 Vere-Jones, D., and Ozaki, T.: Some examples of statistical estimation applied to
445 earthquake data, *Annals of the Institute of Statistical Mathematics*, 34, 189-207, 1982.

446 Wang, J. P., Huang, D., and Chang, S. C.: Assessment of seismic hazard associated with
447 the Meishan fault in Central Taiwan, *Bull. Eng. Geol. Environ.*, 72, 249-256, 2013.

448 Wang, J. P., Lin, C. W., Taheri, H., and Chen, W. S.: Impact of fault parameter
449 uncertainties on earthquake recurrence probability by Monte Carlo simulation – an
450 example in central Taiwan, *Eng. Geol.*, 126, 67-74, 2012.

451 Weichert, D. H.: Estimation of the earthquake recurrence parameters for unequal
452 observation periods for different magnitudes, *Bull. Eng. Geol. Environ.*, 70, 1337-
453 1346, 1980.

454 Yakovlev, G., Turcotte, D. L., Rundle, J. B., and Rundle, P. B.: Simulation-based
455 distributions of earthquake recurrence times on the San Andreas fault system, *Bull.*
456 *Seismol. Soc. Am.*, 96, 1995-2007, 2006.

Table 1. Summary of the model parameters used in the analyses

Parameters	Focal depth (km)	Unit Weight (kN / m ³)	Cohesion (MN / m ²)	Friction angle (degrees)	Return period (years)	<i>K</i> *	<i>n</i> **
Range	4 ~ 8	25 ~ 30	3.6 ~ 22.7	22 ~ 46	112 ~ 212 (162 ± 50) 62 ~ 262 (162 ± 100)	0.2 ~ 0.5	0.25 ~ 1.0
Average	6	27.5	13.2	34	162	0.35	0.63

* *K* = the coefficient of lateral earth pressure in rock; ** *n* = the coefficient of variation for annual stress increment

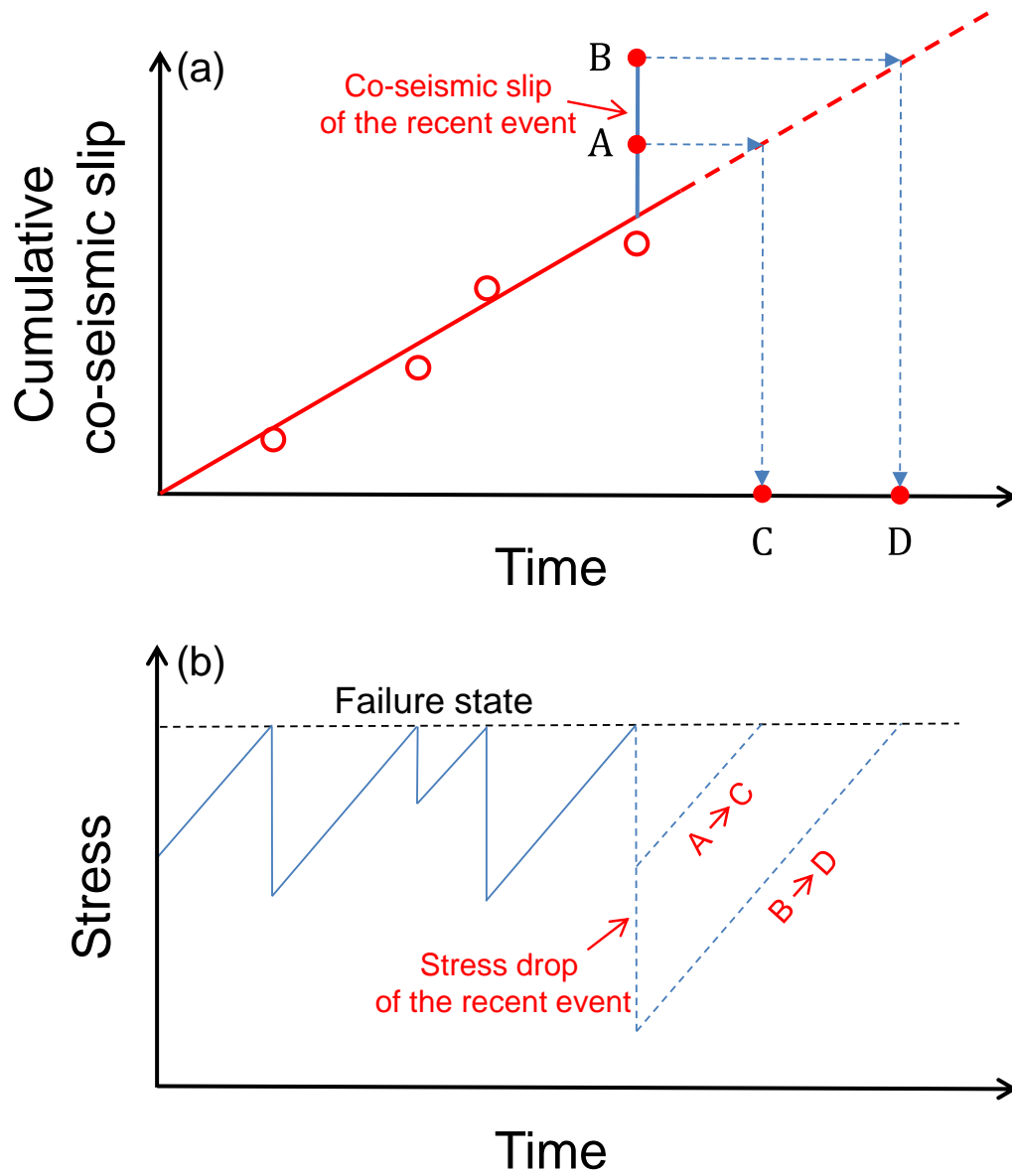


Fig. 1 Schematic diagram for the time-predictable model: a) best-estimate relationship between cumulative co-seismic slips and time, and b) the earthquake-time prediction facilitated with a failure state and a constant stress increment

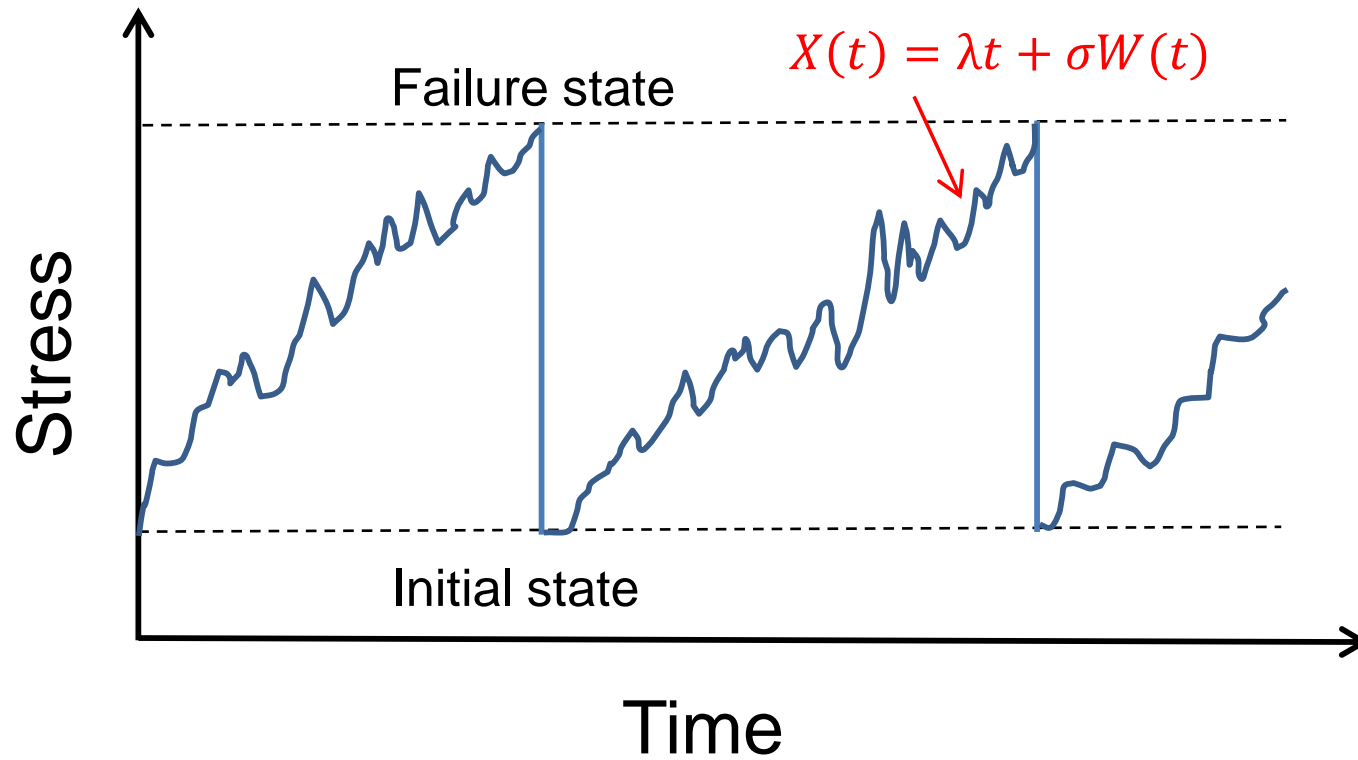


Fig. 2 Schematic diagram showing the essential of the Brownian model; within the two imaginary stress states, the model considers the stress-time series should be random and could be modeled by a long-term stress increment and a Brownian motion as $X(t) = \lambda t + \sigma W(t)$, where $X(t)$ is the stress at time t , λ is long-term stress increment rate, σ is the magnitude of a Brownian motion $W(t)$.

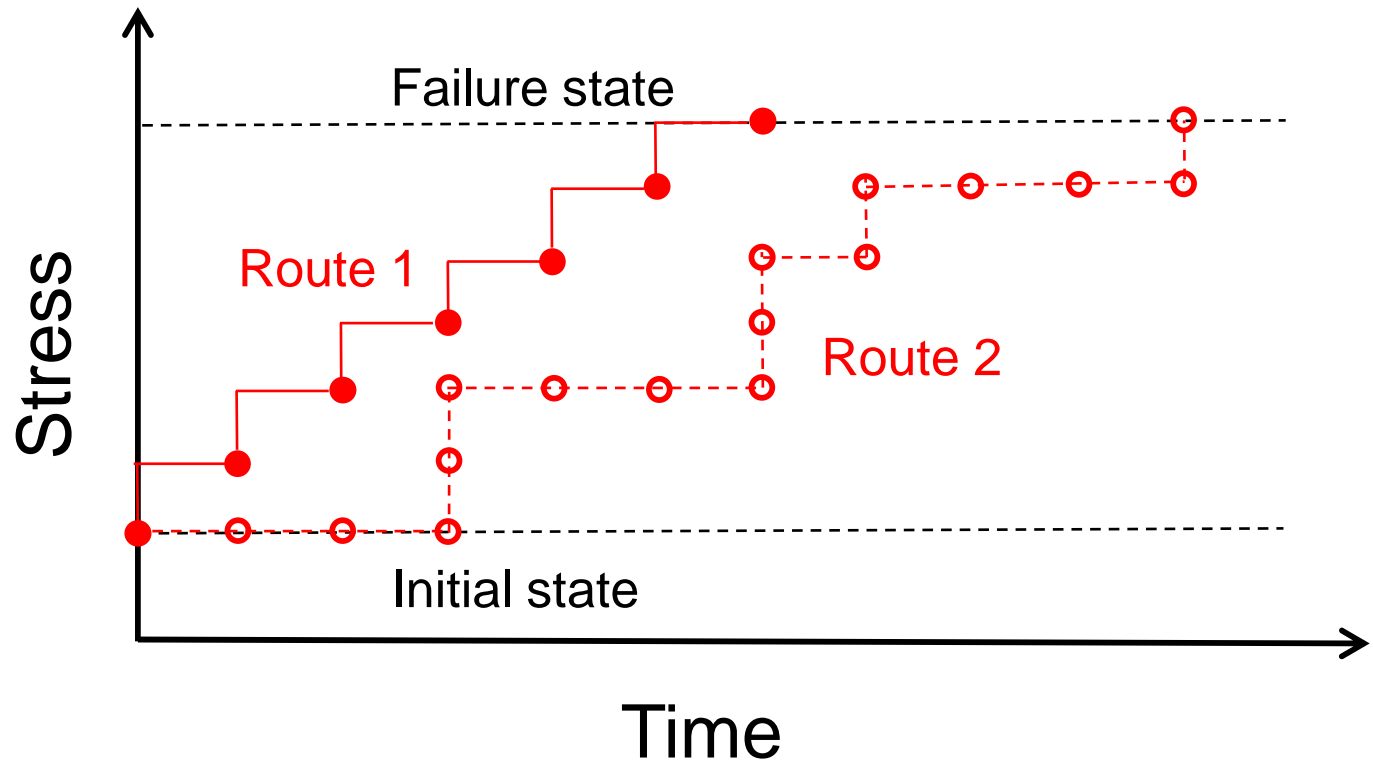


Fig. 3 Schematic diagram illustrating the negative binomial model; between the two stress states, many “stress routes” can be present, and the probability of each route can be estimated with the model, then developing the probability distribution for the interval between two consecutive events

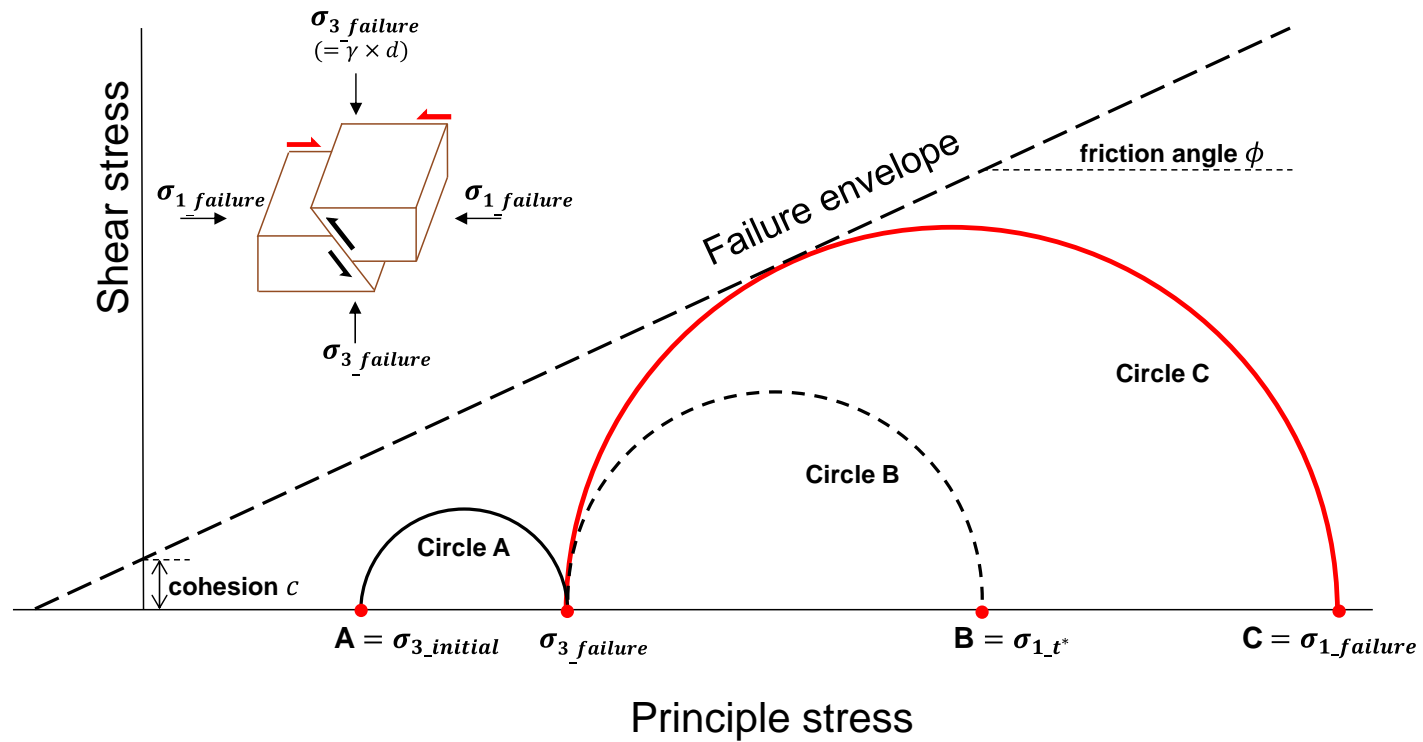


Fig. 4 Schematic diagram illustrating Mohr-Coulomb failure criterion; Circle A represents the initial state after a thrust-fault earthquake or at t_0 , Circle B denotes stress states at t^* after t_0 , and Circle C is the stress state corresponding to the failure state that causes rock failure and earthquake

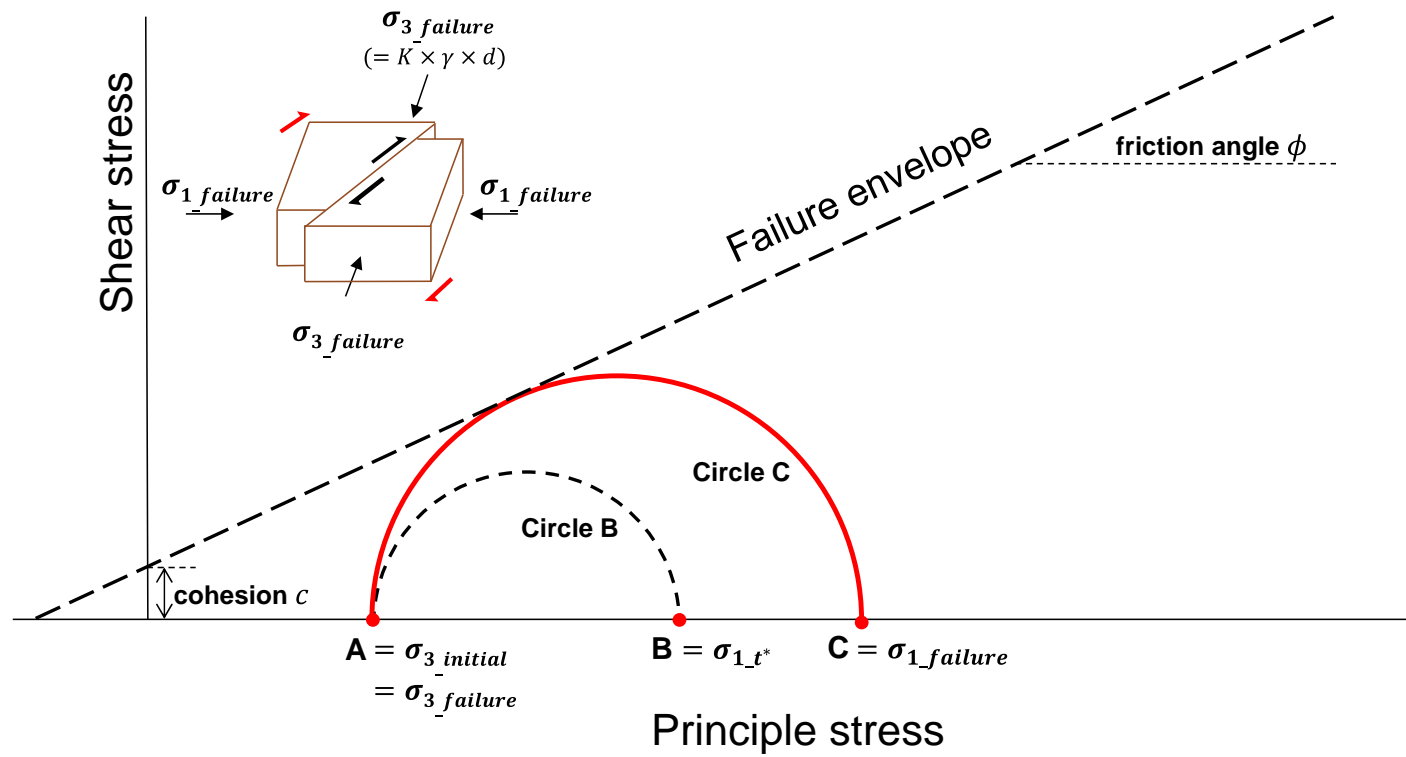


Fig. 5 The Mohr circles for evaluating the non-stationary earthquake probability for strike-skip earthquakes

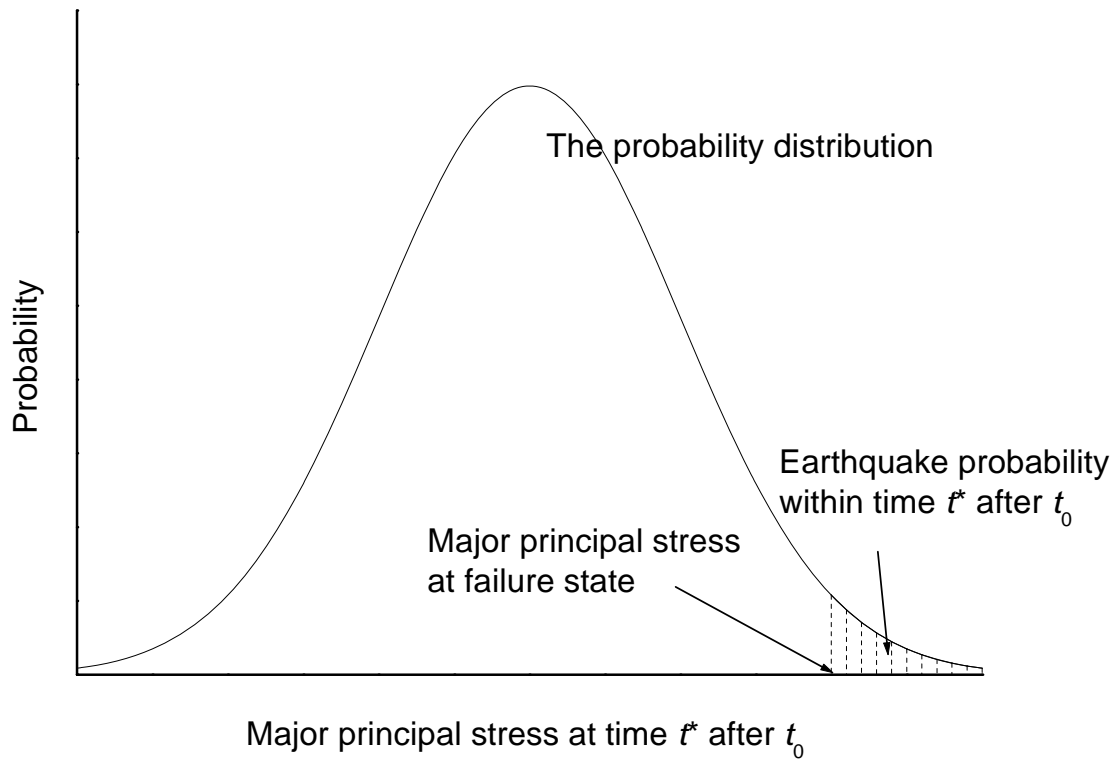


Fig. 6 The essentials of the new non-stationary model: Developing the probability distribution of the major principal stress at time t^* (i.e., $\sigma_{1_{t^*}}$) after the last event or after t_0

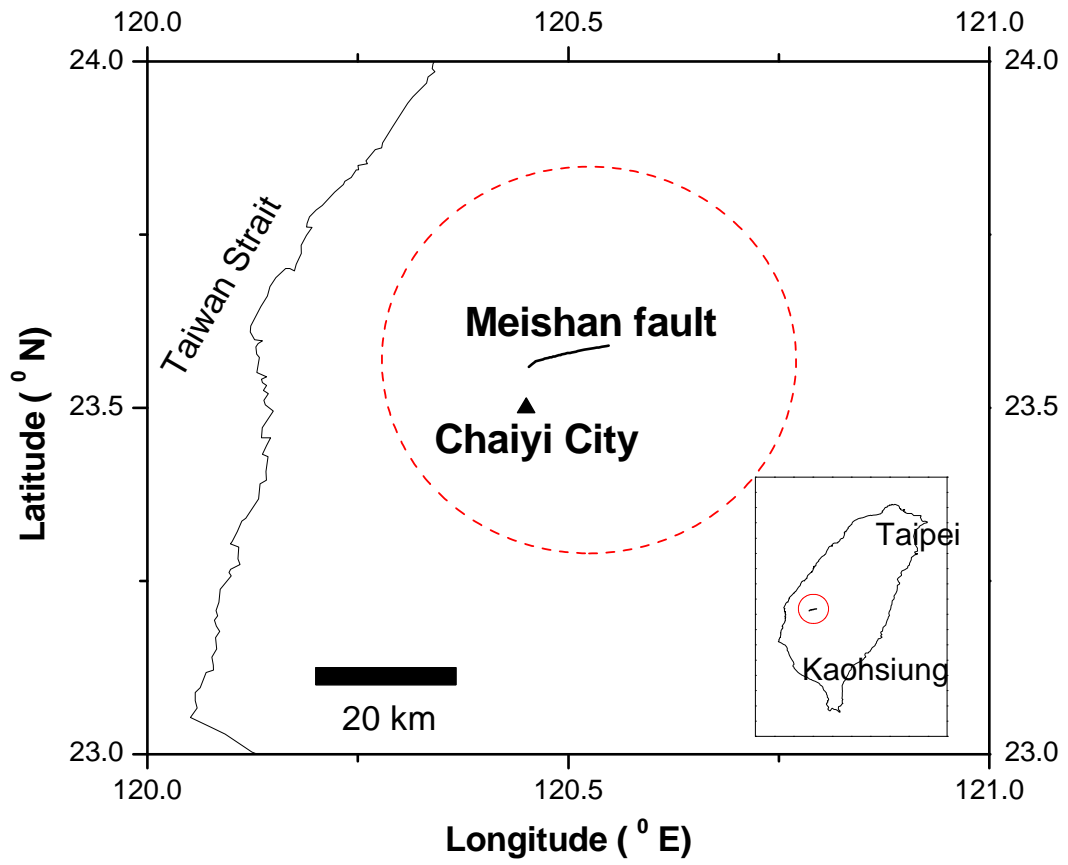


Fig. 7 The location of the Meishan fault in central Taiwan

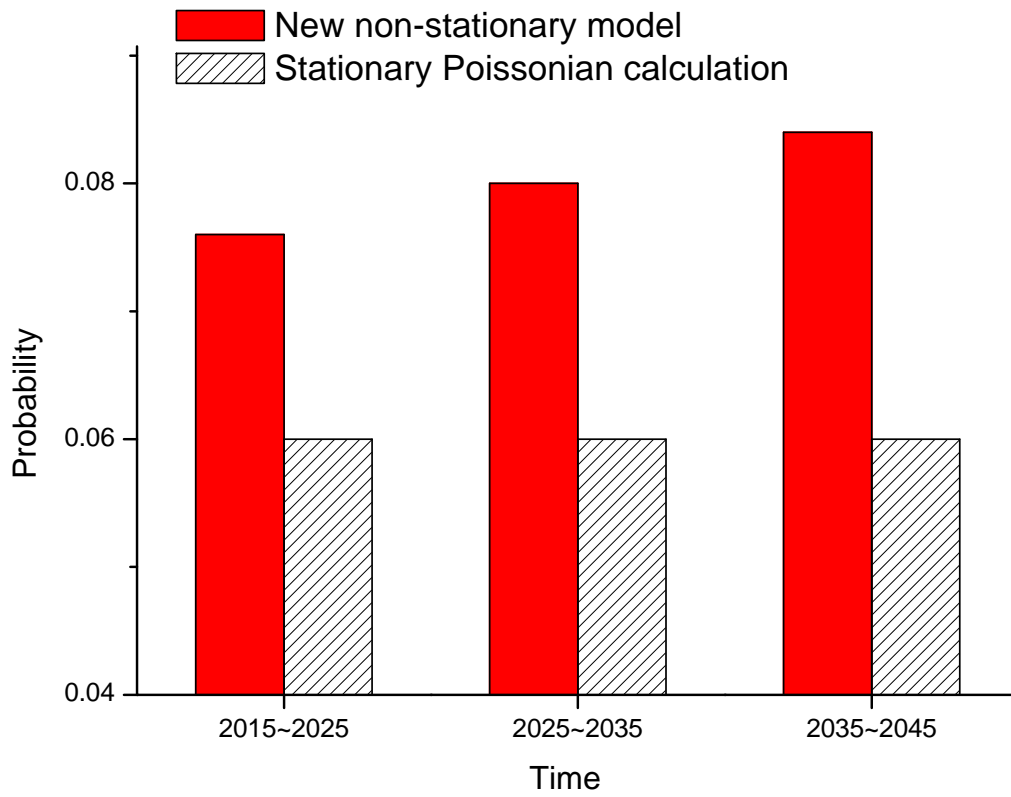


Fig. 8 The earthquake probability associated with the Meishan fault in three 10-year periods subject to the best-estimate return period of 162 ± 50 years (other input data are summarized in Table 1)

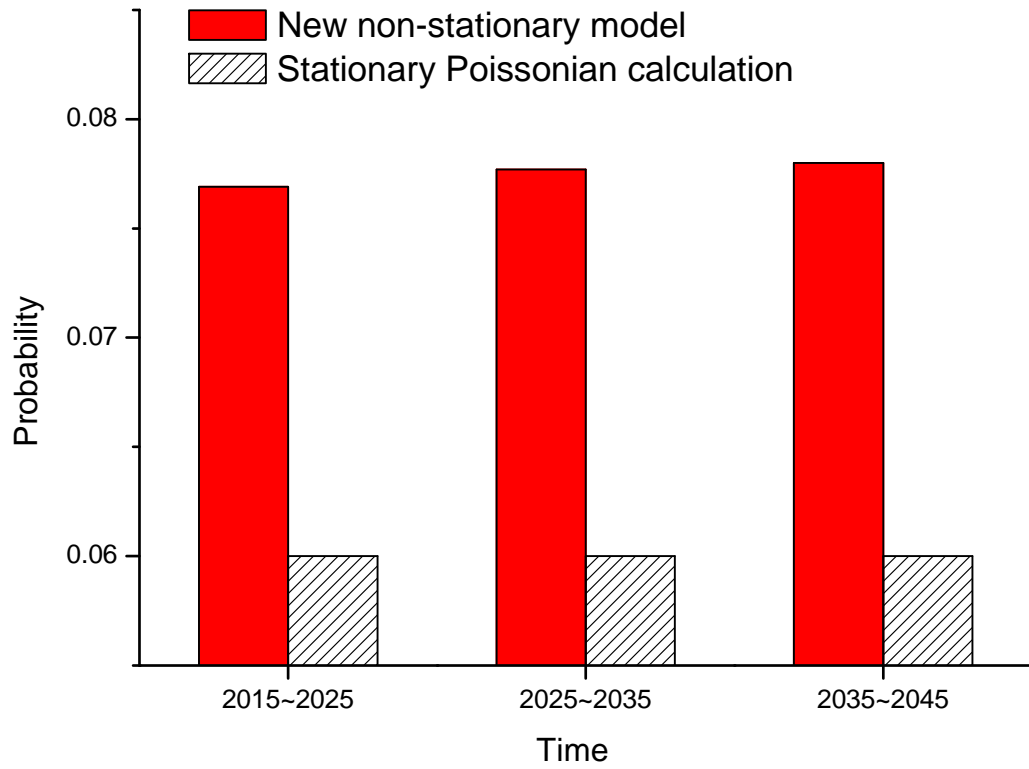


Fig. 9 The earthquake probability associated with the Meishan fault in three 10-year periods subject to the best-estimate return period of 162 ± 100 years (other input data are summarized in Table 1)

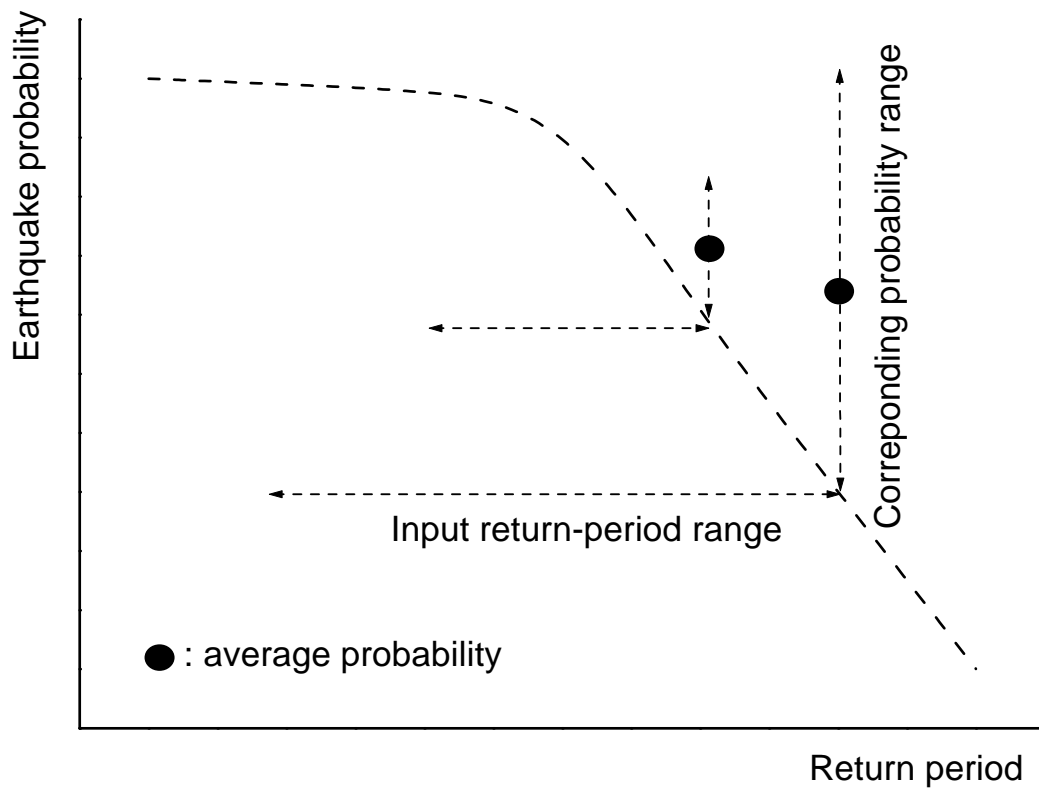


Fig. 10 A schematic graph explaining the average earthquake probability for the model application is decreased with a bigger range of return period, owing to the non-linear relationship between earthquake probability and return period

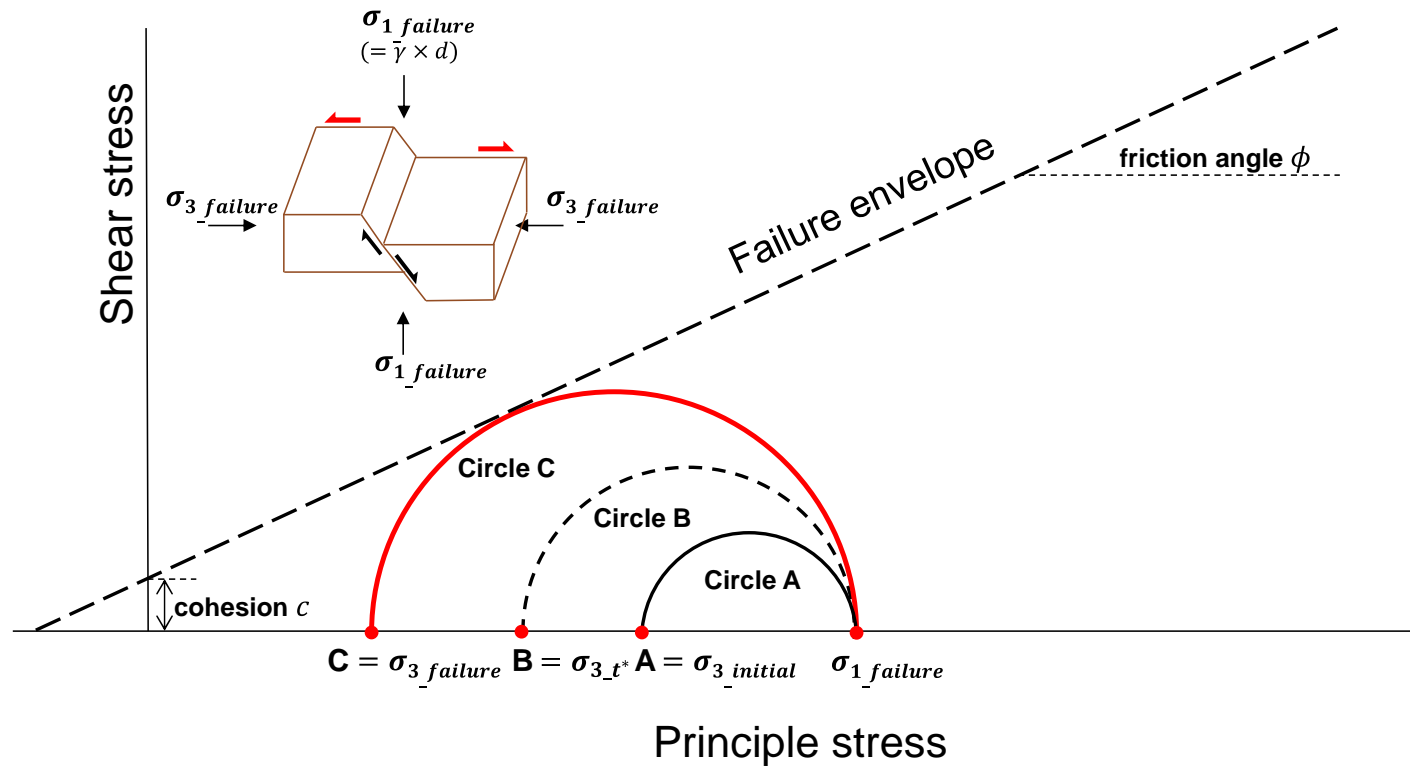


Fig. 11 The Mohr circles for evaluating the non-stationary earthquake probability for normal-fault earthquakes

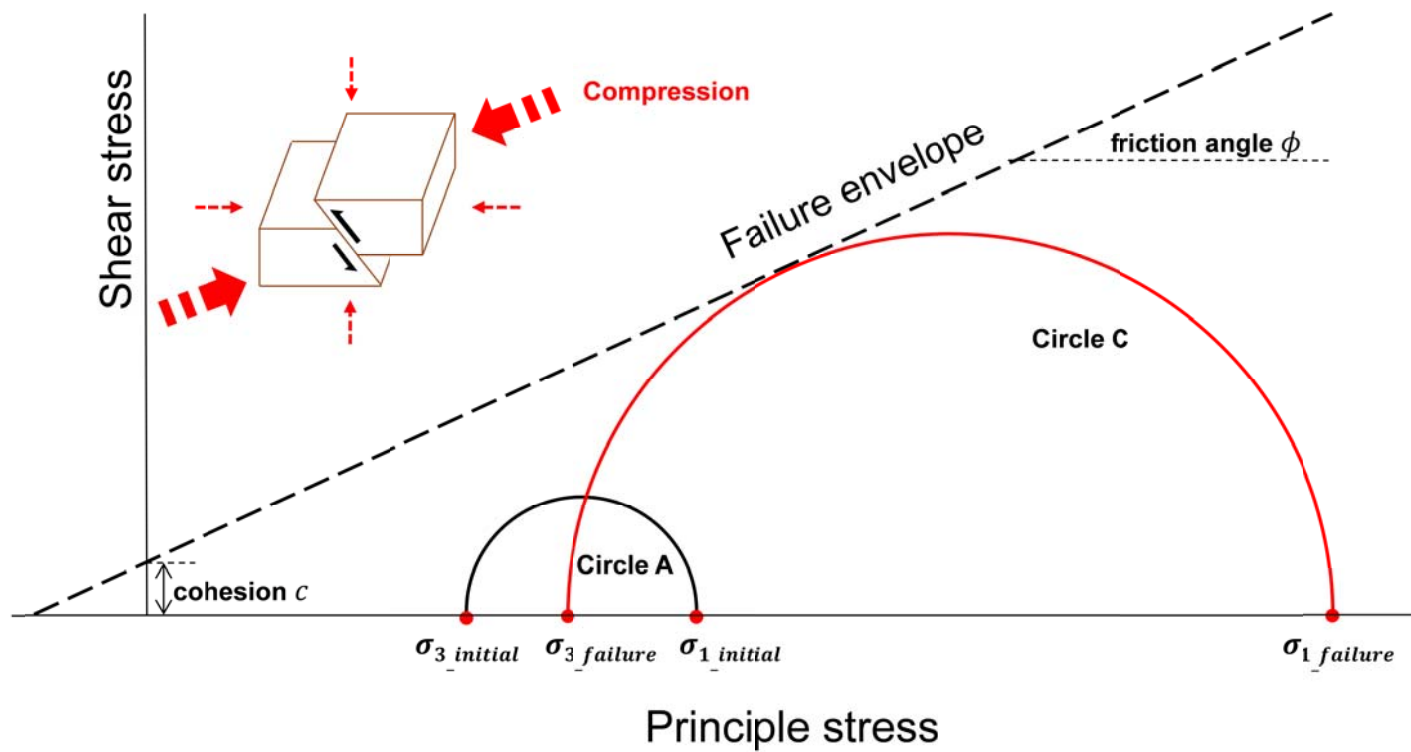


Fig. 12 The Mohr circles for evaluating the non-stationary earthquake probability subject to an oblique tectonic compression

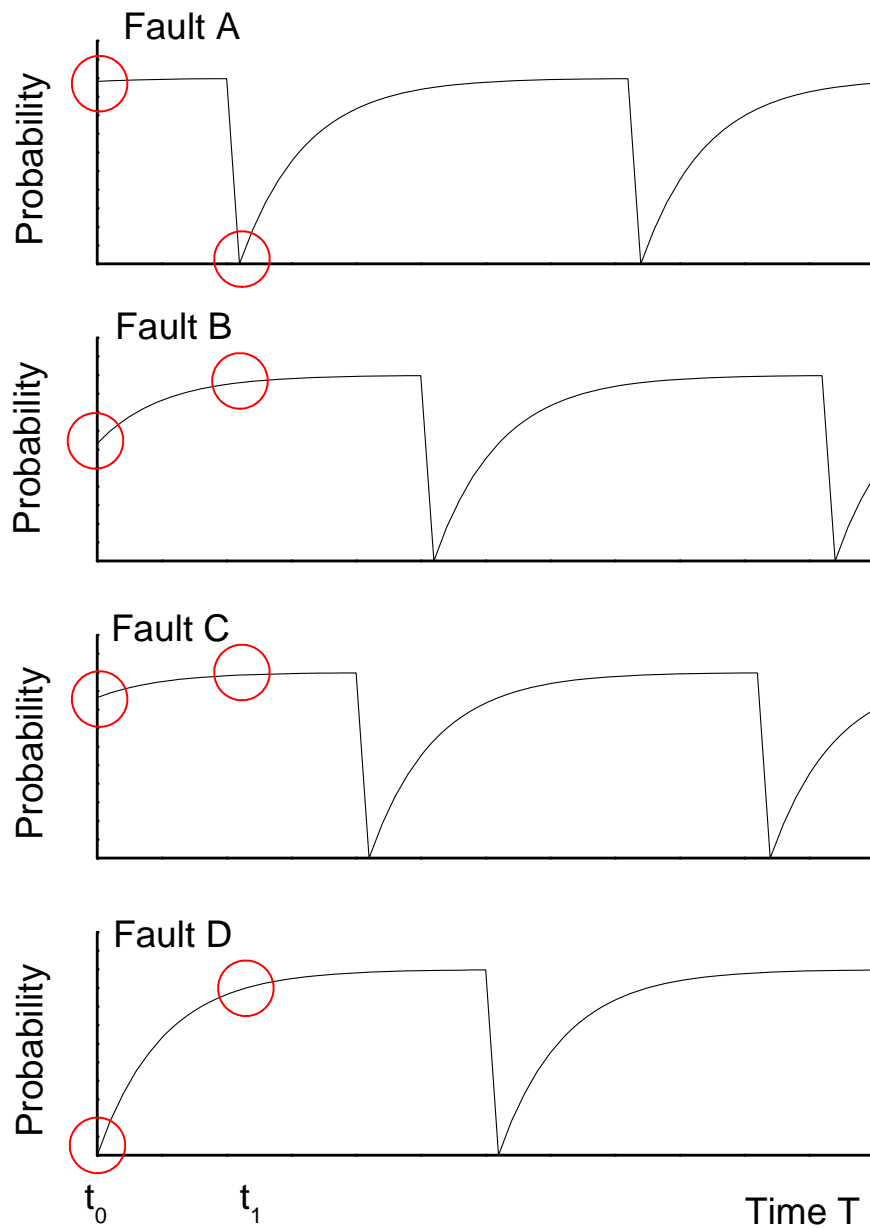


Fig. 13 Schematic diagram illustrating the stationary process after combining many non-stationary processes; taking $T = t_0$ and $T = t_1$ for example, the sum of that many non-stationary probabilities will be close to each other, although the probability is very low for Fault D at $T = t_0$, and it is very low for Fault A at $T = t_1$

Dear Editor Dr. Malamud, the anonymous reviewer, and reviewer Dr. Chan of NTU:

We thank you so much for providing us the valuable comments and suggestions, making our work much improved in so many aspects after revising. The point-by-point comment and response are given in the following. Moreover, for a better trace of our changes and responses in the revision, an annotated revision was attached at the end of this document.

Here, we would like to highlight the novelty of our study as follows: **the new non-stationary earthquake probability assessment from the concepts of Mohr-Coulomb failure criterion**. As receiving only few comments on the model basics and derivations, this novel idea seems agreeable with the Editor and Reviewers. Nevertheless, we endeavored to address other comments as best as we can, such as a more comprehensive literature review and the site-characterization issues in the model application.

Part I: Response to the comments of the anonymous reviewer

Comment 1.1

Discussion of the previous literature on non-stationary earthquake models. The manuscript does a poor job of building on previous non-stationary EQ models, with the latest one mentioned (in the introduction) from 1984. I would expect a much more thorough mention of non-stationary EQ models developed in the last 30 years, so it is clear that the present manuscript is BUILDING on these models, and proposing something different, rather than stating it has not been done.

Response:

The comment is highly appreciated and followed.

In the revision, a more comprehensive review on non-stationary models was given in Section Two. Please see **lines 45-108 and Figs. 1-3** of the annotated revision attached in the end.

Comment 1.2

Size of earthquake considered. Throughout the manuscript, there are words like "EQ after t years since last occurrence" or other such language. I realize that the actual model uses other parameters to give an idea of energy released, but can the entire manuscript be gone over to

put 'size' of the earthquake in context in the language used (or energy released, or other measure).

Response:

We followed the comment in the revision as much as possible, with our best understanding and interpretation on the comment “whether the new model can somehow predict earthquake magnitude or energy release when the event recurs.”

Our responses to “the comment” were added in lines 236-243 of the revision. Basically, like other temporal earthquake analyses, our non-stationary assessment is to estimate the earthquake probability in a given period of time, while it cannot estimate earthquake magnitude or energy release when the event recurs.

(We apologize if the response went to a wrong direction. In case that happens, we would like the reviewer to elaborate the comment a little bit more, so that we can, and will, re-address it in the next revision.)

Comment 1.3

Aftershocks, foreshocks, main shock. Please include brief discussion of how these are included/not included in the model.

Response:

Comment followed. The discussion was given in lines 230-235 of the revision.

Comment 1.4

[Minor] It would be beneficial to add a figure of the Meishan fault and its surroundings.

Response:

Comment followed. Please see lines 261-263 and Fig. 7 of the revision.

Comment 1.5

[Minor] Please be clear in symbols, of ML vs. MW vs. other types of magnitude. I was actually surprised to see ML (local magnitude) being used for the earthquake in question.

Response:

Comment followed. Moment magnitude (M_w) was adopted while preparing the revision, such as in lines 249 - 251.

Comment 1.6

[Minor] Please add a table of variables used, and where they are introduced, as there are a lot of them.

Response:

Comment followed. A section of Notation was added in the revision. Please see lines 140 and 396 of the revision.

• **The summary of response Part I**

Comment	Locations in the revision
1.1	Lines 45-108, Figs. 1-3
1.2	Lines 236-243
1.3	Lines 235-240
1.4	Lines 261-263, Fig. 7
1.5	Lines 249-251
1.6	Lines 140 and 396

***** End of Part I

Part II: response to the comments of Dr. Chan

Comment 2.1

In this manuscript, the authors developed a new physics-based approach for earthquake forecasting and implemented to the Meishan Fault. The approach might be beneficial for subsequent studies on seismic hazard assessment. This work is interesting and the manuscript is well written. I have some comments, which are detailed in the attached file.

Response

The support is highly acknowledged.

Comment 2.2

Table 1, I am very surprised that there is no uncertainty for return period. Thus, the authors assumed that each earthquake is characteristic with identical stress release. However, many of theoretical models and observations disagree the assumptions. For example, after the 2011 Tohoku earthquake, the occurrence of events with normal mechanism suggests coseismic stress drop are larger than the accumulated stress loading. In addition, the return period along the Meishan Fault between the last two events (1792 and 1904) is 113 year, which is not consistent with the assumption.

Response

The comment is highly appreciated, and the summary of the response is as follows:

- a) The reason we used the return period as 162 years in the manuscript is based on the literature. In the revision, we followed the suggestion then using the return periods as 162 ± 50 years and 162 ± 100 years in the model application. However, it must be noted that the “uncertainties” (i.e., ± 50 and ± 100) are from our best judgments.
- b) We could not find the sources of “1792 and 1904 years” of the comment. As a result, our best-estimate return periods as 162 ± 50 and 162 ± 100 years were still based on an “average” value of 162 years from the literature.
- c) Please see **lines 275-279 and Table 1** of the annotated revisions attached in the end.

Comment 2.3

The assumed parameters listed in Table 1 are mainly based on the references for general description of the parameters. It is desired to obtain specific parameters for the Meishan Fault and neighboring regional tectonic regime so that the uncertainty of the result might be minimized. Alternatively, application to other fault system with better investigation, e.g., the Chelungpu Fault, might provide a better demonstration for this approach.

Reponses:

Comment highly appreciated; the summary of the response is as follows:

- a) The reason we used the Meishan earthquake as the application of the new non-stationary model is owing to its imminent earthquake risk. Moreover, the return period of the Meishan fault should be better characterized than other characteristic earthquakes in Taiwan, as used by a few recent studies.
- b) Although the Chelungpu Fault is geologically well-investigated as commented, the fault's "rock mechanics" properties, such as the fault-plane strength parameters, the coefficient of lateral earth pressure in rock, and variability in stress annual increment, are not clear either, even for those geologically, well-investigated faults.
- c) As mentioned in the beginning of the document, the novelty of the study is the new non-stationary earthquake probability assessment. Certainly, we also hope to see more studies focusing on site characterizations that could improve the reliability of an application as the model is used. However, this "huge" task is not within the scope of the study, aiming to develop a new non-stationary earthquake analysis.
- d) Please **lines 252-260, 266-285, and 322-342** of the revision for the response.

Comment 2.4

It is known that the Meishan Fault as well as the 1906 earthquake is with strike-slip mechanism, i.e., both maximum (σ_1) and minimum (σ_3) principal axes are horizontal. I am not quite sure if the fault with strike-slip mechanism also fulfils the assumption of equation (7).

Responses

Comment followed. More statements were added in the revision to clarify that the non-stationary analysis is applicable to the three types of earthquake. Please see **lines 158-163, 345-352, Figs. 5 and 11** of the revision.

Comment 2.5

In ‘3 The Poisson process and earthquake probability’, I agree that the Poisson model is a stationary function. However, I expect the equation (2) and (3) are unnecessary since they are identical to equation (1).

Response:

Comment followed. The two equations were deleted in the revision.

Comment 2.6

Table 1, earthquake depth is a crucial parameter for the approach. However, I am confused if it is defined by hypocentral depth or rupture depth. In addition, according to field survey, the Meishan Fault obtains surface rupture, i.e., the range should be as shallow as 0 km.

Response:

The depth refers to the focal depth, and it was more clearly stated throughout the revision, such as in lines 13, 226, 390, 396, etc...

Comment 2.7

Table 1, I expect the authors want to express ‘Median value’ instead of ‘Central value’.

Response:

Comment followed. The central value was changed to “average.”

• **Summary of Responses Part II**

Comment	Locations in the revision
2.1	The support is acknowledged.
2.2	Lines 275-279
2.3	Lines 252-260, 266-285, and 322-342
2.4	Lines 158-163, 345-352, Figs. 5 and 11
2.5	Deleted in the revision
2.6	Lines 13, 226, 390, 396, etc...
2.7	Table 1

***** End of Response Part II

Finally, we would like to thank you again for the valuable comments on the submission. We hope the responses satisfactorily address your concerns. If not, we are more than glad to make more revisions and explanations in the next round of revision.

Sincerely,

J.P. Wang

&

Yun Xu

Attachment: the annotated revision

Annotated Revision

1 **A non-stationary earthquake probability assessment with Mohr-Coulomb failure**
2 **criterion: including an application to central Taiwan**

3
4 **Abstract:** From theory to experience, earthquake probability associated with an active
5 fault should be gradually increasing with time since the last event. In other words, the
6 process should be non-stationary, rather than being stationary as the Poisson process. In
7 this paper, a new non-stationary earthquake assessment is introduced. Different from
8 other analyses, the new model more clearly defines and calculates two stress states or
9 boundary conditions between two consecutive earthquakes, facilitated with the Mohr-
10 Coulomb failure criterion. In addition to the model development, this paper also presents
11 a model application to evaluate earthquake probability associated with the Meishan fault
12 in central Taiwan. Based on the best-estimate return period of 162 ± 50 years, focal
13 depth of 4 ~ 8 km, etc., there could be a 7.6% probability for the fault to induce a major
14 earthquake in years 2015 ~ 2025, and if the earthquake does not recur by 2025, the
15 earthquake probability will increase to 8% in 2025 ~ 2035, a non-stationary probability
16 depending on the starting dates of a given period of time.

R2.6

17
18 **Keyword:** non-stationary earthquake probability assessment, Mohr-Coulomb failure
19 criterion

20
21 J.P. Wang; Dept Civil & Environmental Engineering, Hong Kong University of Science and
22 Technology, Kowloon, Hong Kong

23 Yun Xu; Dept Civil & Environmental Engineering, Hong Kong University of Science and
24 Technology, Kowloon, Hong Kong

24 **1. Introduction**

25 Owing to our imperfect understandings and natural randomness of earthquake,
26 several models have been proposed for estimating earthquake probability in a given
27 period of time. Among them, the Poisson model might be the one that is mostly used in
28 many applications (e.g., Weichert, 1980; Ang and Tang, 2007; Ashtari Jafari, 2010).
29 However, it must be noted that the Poisson calculation is a “memory-less” model (Devore,
30 2008), meaning that the Poissonian probability is only a function of length of time, but
31 irreverent to when the last earthquake was occurring.

32 However, it seems that the recurrence of a characteristic earthquake associated
33 with a given active fault should not be stationary or memory-less. That is, the earthquake
34 probability should be gradually increasing with time. Taking the recent Nepal earthquake
35 in April 2015 for example, the probability for the very next Nepal earthquake to recur in
36 2015 ~ 2020 should be lower than that in 2115 ~ 2120, although the two have the same
37 length of time.

38 The scope of this study is to develop a new non-stationary earthquake probability
39 assessment, mainly from the concepts of the Mohr-Coulomb failure criterion. Meanwhile,
40 this paper provides a comprehensive review on other non-stationary earthquake models
41 (Section Two), followed by our non-stationary analysis (Section Three). Then, the new
42 model was demonstrated with a model application to central Taiwan (Section Four), as
43 well as model improvement and future work (Section Five).

44

45 **2. An overview of non-stationary earthquake models**

R 1. 1

46 In this section, we would like to provide a comprehensive review on non-
47 stationary earthquake analyses and models. Specifically, we characterized the models
48 into two groups, referred to as “statistical models” and “physical model.”

49

50 2.1 Statistical models

51 Basically, those statistical models developed are more or less a derivative of the
52 stationary Poisson model. For example, Vere-Jones and Ozaki (1982) proposed the use
53 of a time-variant model parameter for the Poissonian calculation, making their model
54 non-stationary although the calculation is still Poissonian in essence. Similarly, another
55 work suggested the use of adjusted return period (related to current time and original
56 return period) for the Poissonian calculation, in order to modify the Poisson model from
57 stationary to non-stationary (Wang et al., 2013).

58 Another type of modification is to use non-exponential distributions to model
59 earthquake inter-occurrence time intervals as a random variable. (Note that for an event
60 modeled by a Poisson process, the number of events in a given period of time is a discrete
61 random variable following the Poisson distribution; meanwhile the time when the next
62 event would recur is a continuous variable following the exponential distribution.) For
63 example, the log-normal distribution (Ferrás, 2005), Weibull distribution (Yakovlev et
64 al., 2006), and Gamma distribution (Gómez and Pacheco, 2004) have been suggested for
65 the replacement of the exponential distribution, with them all featuring a non-stationary
66 analysis after such modifications.

67 Based on given earthquake data, it must be noted that the statistical models are all
68 empirical in a sense. In other words, the models are in no consideration of earthquake
69 mechanisms, such as tectonic stress accumulation under the ground.

70

71 2.2 Physical models

72 In consideration of earthquake mechanics, several non-stationary earthquake
73 analyses have also been proposed from a different perspective. It must be noted that the
74 models are not entirely a “product” of physics, but somehow on the basis of the concepts
75 of physics working together with empirical models. Specifically, we would like to
76 introduce three of them in the following that are more related to our non-stationary
77 earthquake model.

78 The first one we like to introduce here is the time-predictable model (Shimazaki
79 and Nakata, 1980). Fig. 1 is a schematic diagram illustrating the model basics.
80 Essentially, the model is relying on a best-estimate relationship between co-seismic fault
81 slip (or displacement) and time. For instance, given the last event with fault slips as
82 Points A and B (see Fig. 1), then the next event should recur at the time of Points C and
83 D. In other words, the recent event with a smaller fault slip should accompany a smaller
84 stress drop, and under a constant stress increment with time, it should lead to a shorter
85 time for the stress to re-reach a stress level (or failure stress state) that could induce
86 earthquakes.

87 The next model of the group is the Brownian model (Ellsworth, 1995; Matthews
88 et al., 2002). By contrast to the time-predictable model, the Brownian model is not on the
89 basis of a constant stress increment, while considering the stress increments between two

90 consecutive events should be a stochastic process like Fig. 2. Specifically, the model
91 considers the stress-time series is a combination of a long-term stress increment and a
92 Brownian motion simulating transient stress randomness. With such a function, we can
93 estimate the time of the next earthquake by examining if the stress reaches the failure
94 state within a given period of time.

95 The third one we like to introduce is the negative binomial model (Tejedor et al.,
96 2015). As the previous analyses, the model is also on the basis of two imaginary stress
97 states. As shown in Fig. 3, the essence of the model is that the stress change in unit time
98 could be modeled by two scenarios: stress does and does not increase. As a result, there
99 are many possible “stress routes” (as shown in Fig. 3) between two consecutive events,
100 and the probability and the total time of each route could be calculated with given
101 earthquake return periods. Finally, the inter-occurrence time interval can be derived as a
102 negative binomial distribution for such a non-stationary probability assessment.

103 To sum up, the three physical models are all facilitated with two stress states that
104 are part of the earthquake occurrence theories generally accepted. Somehow, we do
105 share this perspective for our model development. However, the biggest difference is
106 that our model defines and calculates the two stress states more clearly, on the basis of
107 the Mohr-Coulomb failure criterion that is well established and used in rock mechanics,
108 structural geology, etc.

109

110 **3. The new non-stationary earthquake probability assessment**

111 3.1 Overviews of Mohr-Coulomb failure criterion and elastic rebound theory

112 The Mohr-Coulomb failure criterion is a model describing the response of
113 materials subject to external stresses (Pariseau, 2007), and it was commonly applied to
114 rock mechanics as well as other applications. Fig. 4 is a schematic diagram illustrating
115 the essentials of the model. Basically, as the Mohr circle is below the failure envelope, a
116 shear failure is not expected in the material. By contrast, as long as the Mohr circle is in
117 contact with the failure envelope, a shear failure could occur.

118 On the other hand, it is generally accepted that the ongoing tectonic activities are
119 the main reason causing rock failures under the ground, resulting in an earthquake with
120 the release of accumulated strain energy. Afterward, the energy re-accumulates and re-
121 releases until the next earthquake, and such a theory is referred to as the elastic rebound
122 theory (Keller, 1996), proposed by Reid in the early twentieth century (Reid, 1910).

123

124 3.2 The model basics and the algorithms

125 The two earthquake theories above were mainly the motivation of the new non-
126 stationary model: 1) based on the Mohr-Coulomb failure criterion, the rock subject to the
127 stress state as Mohr Circle C (see Fig. 4) should fail and cause an earthquake, at which
128 we refer to it as failure state; 2) from the elastic rebound theory, the stress state in the
129 rock right after a characteristic earthquake should be restored to Mohr Circle A, which is
130 called the initial state at time t_0 .

131 As a result, the problem to evaluate the earthquake probability within a given time
132 t^* after the last event (or after t_0) is becoming a problem as follows: What is the chance
133 for the major principle stress at time t^* (denoted as $\sigma_{1_{t^*}}$) greater than the major principle

134 stress at the failure state (denoted as $\sigma_{1_failure}$)? Or the question can be mathematically

135 expressed by the following equation:

136

137
$$\Pr(\text{earthquake within } t^* \text{ after } t_0) = \Pr(\sigma_{1_t^*} > \sigma_{1_failure}) \quad (1)$$

138

139 Clearly, the problem now is governed by two variables $\sigma_{1_t^*}$ and $\sigma_{1_failure}$, and their

140 relationships with other parameters will be detailed later. Note that those notations used

141 in the following derivations are summarized in the end of the paper.

R1.6

142

- 143 • The major principle stress at failure state, $\sigma_{1_failure}$

144 Based on the Mohr-Coulomb failure criterion, the major principal stress at failure

145 state (Point C in Fig. 4) can be expressed as a function of the minor principal stress at

146 failure ($\sigma_{3_failure}$), and two strength parameters of the shearing plane, i.e., cohesion c and

147 friction angle ϕ (Pariseau, 2007):

148

149
$$\sigma_{1_failure} = \sigma_{3_failure} \left(\frac{1 + \sin \phi}{1 - \sin \phi} \right) + \frac{2c \times \cos \phi}{1 - \sin \phi} \quad (2)$$

150

- 151 • The minor principal stress at failure state, $\sigma_{3_failure}$

152 The minor principal stress at failure is attributed to the overburden earth pressure

153 above the focal depth d , which can be estimated with the following formula based on

154 rock mechanics:

155

156 $\sigma_{3_failure} = \gamma \times d$ (3)

157

158 where γ is rock unit weight. It must be noted that this model considers $\sigma_{3_failure}$ as time-
159 invariant (more discussion is given later), and the case shown in Fig. 4 and Eq. 3 is for a
160 thrust-fault earthquake. As for the strike-slip fault, the Mohr circles of the initial state
161 and the failure state are shown in Fig. 5, indicating $\sigma_{3_failure}$ is equal to $\gamma \times d \times K$ for this
162 case, where K is the coefficient of lateral earth pressure in rock. More discussion over
163 model improvements is given in Section 5.2.

R2.4

164

- 165 • The major principle stress at time t^* , $\sigma_{1_t^*}$

166 With tectonic stress increasing with time, the key task of the new analysis is to
167 estimate the major principle stress at time t^* after the last event. For thrust-fault
168 earthquakes as those Mohr circles shown in Fig. 4, the major principle stress at time t^*
169 can be formulated as follows:

170

171 $\sigma_{1_t^*} = \sigma_{3_initial} + t^* \times ASI$ (4)

172

173 where $\sigma_{3_initial}$ is the minor principal stress at the initial state (or at t_0) and ASI is called
174 annual stress increment. Note that from Fig. 4 (the thrust fault) and Fig. 5 (the strike-slip
175 fault), $\sigma_{3_initial}$ is equal to $\gamma \times d \times K$ for the two cases of the non-stationary analysis.

176

177 3.3 The return period \tilde{t} and its relationship with $\sigma_{1_{t^*}}$

178 In addition to γ, d, K , etc., the return period \tilde{t} of characteristic earthquakes is
179 another input data of the non-stationary analysis. Moreover, the mean value and standard
180 deviation of $\sigma_{1_{t^*}}$ can be expressed as a function of \tilde{t} , and used for developing its
181 probability density function for the non-stationary probability assessment within the
182 given time t^* .

183 From the meaning of return period, it is understood that the event will recur when
184 return period \tilde{t} is due. As a result, the major principal stress at return period \tilde{t} (denoted
185 as $\sigma_{1_{\tilde{t}}}$) should be equal to $\sigma_{1_{failure}}$:

186

$$187 \quad \sigma_{1_{\tilde{t}}} = \sigma_{3_{initial}} + \tilde{t} \times ASI = \sigma_{1_{failure}} \quad (5)$$

188

189 Therefore, the mean value of ASI (denoted as μ_{ASI}) can be derived as follows:

190

$$191 \quad E[\sigma_{1_{failure}}] = E[\sigma_{3_{initial}} + \tilde{t} \times ASI] \quad (6)$$

$$\Rightarrow E[ASI] = \frac{\sigma_{1_{failure}} - \sigma_{3_{initial}}}{\tilde{t}} = \mu_{ASI}$$

192

193 where $E[]$ denotes the mean value of a variable in probability and statistics.

194 On the other hand, as the variability of annual stress increment is equal to n in
195 terms of coefficient of variation (= standard deviation / mean value), its standard
196 deviation (denoted as s_{ASI}) can be derived as follows with its mean value from Eq. 6:

197

$$198 \quad n = \frac{s_{ASI}}{\mu_{ASI}} \Rightarrow s_{ASI} = n \times \mu_{ASI} = \frac{n \times (\sigma_{1_failure} - \sigma_{3_initial})}{\tilde{t}} \quad (7)$$

199

200 With the mean (Eq. 6) of ASI , we can continue deriving the mean value of the major
201 principal stress at time t^* :

202

$$\sigma_{1_t^*} = \sigma_{3_initial} + t^* \times ASI$$

$$203 \quad \Rightarrow E[\sigma_{1_t^*}] = E[\sigma_{3_initial} + t^* \times ASI] = \sigma_{3_initial} + t^* \times E[ASI] \quad (8)$$

$$= \sigma_{3_initial} + \frac{t^* \times (\sigma_{1_failure} - \sigma_{3_initial})}{\tilde{t}}$$

204

205 Similarly, the standard deviation of the major principal stress at time t^* (denoted as $s_{\sigma_{1_t^*}}$)

206 can be derived as follows with s_{ASI} in Eq. 7:

207

$$\sigma_{1_t^*} = \sigma_{3_initial} + t^* \times ASI$$

$$208 \quad \Rightarrow V[\sigma_{1_t^*}] = V[\sigma_{3_initial} + t^* \times ASI] = t^{*2} \times V[ASI] = t^{*2} \times s_{ASI}^2 \quad (9)$$

$$\Rightarrow s_{\sigma_{1_t^*}} = \sqrt{V[\sigma_{1_t^*}]} = t^* \times s_{ASI} = \frac{t^* \times n \times (\sigma_{1_failure} - \sigma_{3_initial})}{\tilde{t}}$$

209

210 where $V[\]$ denotes variance in probability and statistics, and it is the square of standard
211 deviation.

212 In order to establish the probability density function of $\sigma_{1_{t^*}}$, the information
213 about what probability distribution the variable is following is as essential as its mean
214 value and standard deviation. But since the distribution of $\sigma_{1_{t^*}}$ is unknown (to the best
215 of our knowledge, no study has ever worked on the subject), we suggest the normal
216 distribution for this non-stationary earthquake assessment, as it is usually recommended
217 for a probability analysis when the variables' distribution is unknown (Abramson et al.,
218 2002).

219

220 3.4 Summary

221 Fig. 6 is a schematic diagram illustrating the essentials of the non-stationary
222 assessments. The key to the model is to estimate the probability distribution of the major
223 principal stress at time t^* after the last event (or after t_0), and compares it to the stress that
224 could cause rock failures and earthquakes. To sum up, the new non-stationary model is
225 governed by a total of six parameters as follows: return period (\tilde{t}), fault-plane strength
226 parameters (c and ϕ), rock unit weight (γ), earthquake focal depth (d), and the
227 variability of annual stress increment in terms of coefficient of variation (n).

R2.6

228

229 3.5 Presumption and limitation

230 The elastic rebound theory is a plausible explanation to earthquake, but
231 specifically speaking, it is more of a theory about main shocks. As a result, the new non-
232 stationary analysis of the study motivated by such a theory is more applicable to main
233 shocks, a situation similar to other non-stationary models that are also applicable to main

R1.3

234 shocks rather than dependent shocks (Shimazaki and Nakata, 1980; Ellsworth, 1995;
235 Matthews et al., 2002; Tejedor et al., 2015).

236 On the other hand, like any other stationary or non-stationary analyses estimating
237 earthquake probability in a given period of time, our model cannot predict the magnitude
238 of the recurring event, either. In other words, the (earthquake) temporal analyses closely
239 related to return period, stress increment, etc. do not further relate the variables to
240 earthquake magnitudes or energy release. Again, such a framework is similar to other
241 stationary or non-stationary temporal analyses only focusing on the earthquake
242 probability in a given period of time, but not on the probability distribution of earthquake
243 magnitude or energy release when the event recurs.

R1.2

244

245 **4. A model application**

246 **4.1 The Meishan earthquake in central Taiwan**

247 The region around Taiwan is known for high seismicity owing to the location
248 close to the boundaries of tectonic plates. On average, there are around 2,000
249 earthquakes above M_w 3.0 (moment magnitude) occurring around Taiwan every year,
250 with a catastrophic event, like the M_w 6.4 Meishan earthquake in 1906 and the M_w 7.6
251 Chi-Chi earthquake in 1999, that could recur in decades.

R1.5

252 As a result, we would like to apply the new non-stationary model to Taiwan as a
253 case study. Specifically, we selected the Meishan fault in central Taiwan as the model
254 application, given a few recent studies pointing out the fault should be of “imminent”
255 earthquake risk, for the event’s return period being “almost” due (e.g., Wang et al., 2012).
256 By contrast, the reason we did not select the Chelungpu fault as the application is because

R2.3

257 the active fault should be of lower earthquake risk in next couple decades, given it “just”
258 induced the Chi-Chi earthquake in 1999, and should have a longer return period (about
259 250 years) than the Meishan earthquake (Cheng et al., 2007). More discussion over this
260 model application is given in Section 5.1.

261 _____ Fig. 7 shows the location of the Meishan fault in central Taiwan. Accordingly,
262 the fault is very close to a major city (i.e., Chiayi) in central Taiwan, and reportedly the
263 1906 Meishan earthquake killed around 1,200 people in the area.

R1.4

264

265 4.2 The best-estimate data from the literature

266 Table 1 summarizes our best-estimate data from the literature for the non-
267 stationary earthquake assessment on the Meishan fault. It must be noted that because the
268 strength parameters of the fault plane are not clear, we used a typical range (see Table 1)
269 from rock mechanics as our best estimates. Similarly, a probable range of 0.2 ~ 0.5 was
270 used as our best estimate for the coefficient of lateral earth pressure in rock, given no
271 site-specific studies and data have been reported. As for the earthquake focal depth, we
272 considered the depth should be close to 6 km as the last Meishan earthquake (Ng et al.,
273 2009). However, in order to account for the focal-depth uncertainty in the analysis, we
274 used a best-estimate range as 4 ~ 8 km.

R2.3

275 A similar situation was encountered in the determination of the best-estimate
276 return period. On the basis of 162 years used in recent studies (e.g., Wang et al., 2012),
277 two best-estimate ranges were determined as 162 ± 50 years and 162 ± 100 years.
278 Understandably, the uncertainties (i.e., ± 50 and ± 100) are from our best judgments,
279 given such information is not clear from the literature. As for the variability of annual

R2.2

R2-3

280 stress increment, to the best of our knowledge, there is no any research so far that can
281 really answer the question. As a result, the range of 0.25 ~ 1 was used as our best
282 estimate characterizing the variability of annual stress increment in terms of coefficient of
283 variation.

284 More discussion about the input data characterizations and the model application
285 is given in Section 5.1 in the following.

286

287 4.3 Monte Carlo Simulation

288 Because our input data were characterized by a range rather than a single value, it
289 is difficult to solve the governing equation (Eq. 1) of the non-stationary probability with
290 analytical approaches. Therefore, we used Monte Carlo Simulation (MCS) to solve the
291 problem as many MCS applications. For more details about Monte Carlo Simulation,
292 readers can refer to the textbooks of Ang and Tang (2007), Abramson et al. (2002),
293 among many others.

294

295 4.4 The result

296 With the best-estimate input data summarized in Table 1, Fig. 8 shows the
297 average probabilities for three 10-year periods from Monte Carlo Simulation with a
298 sample size of 5,000. For example, the non-stationary model shows a 7.6% probability
299 for the Meishan fault in central Taiwan to induce a major earthquake in years 2015 ~
300 2025, under the return period of 162 ± 50 years. Then, if the event does not recur by
301 2025, the earthquake probability in 2025 ~ 2035 will increase to 8%; similarly, if the
302 event does not recur by 2035, the probability will further increase to 8.4%. Note that the

303 standard deviations of the three probability estimates are all close to 3.3%, which is a
304 reflection to the input data that were characterized by a range. In other words, if the input
305 data were all characterized by single values, the standard deviation of the probability
306 estimates cannot be calculated and reported.

307 In addition, the Poissonian probabilities for the same problem are also shown in
308 Fig. 8. It shows that for a 10-year period of time, the earthquake probability is about 6%
309 for the three different periods (i.e., 2015 ~ 2025, 2025 ~ 2035, and 2035 ~ 2045), or the
310 probability is irrelevant to the starting dates of the time period.

311 Fig. 9 shows the result for the other scenario under return period as 162 ± 100
312 years. Interestingly, the average probabilities for the three 10-year periods become
313 relatively close to one another, and they are smaller than those estimates subject to the
314 return period of 162 ± 50 years. Our explanation to this is as follows: As shown in Fig.
315 10, the relationship between return period and earthquake probability could be highly
316 non-linear. Therefore, the average probability subject to a bigger range of return period
317 would be lower than that subject to a smaller range. Nevertheless, with the non-
318 stationary model, the probability estimates do vary with the starting dates of the time, or
319 the probabilities are indeed non-stationary, in contrast to the stationary Poisson process.

320

321 **5. Discussions**

322 5.1 Input data characterizations

323 As many analyses, input data characterizations are equally challenging as the
324 model development. As a result, for improving the model estimates, we hope to see more
325 studies focusing on site characterizations with more laboratory works or field

R2.3

R2.3

326 instrumentation assessing stress increment variability, fault-plane strength parameters,
327 lateral earth pressure in rock, etc. However, this is beyond the scope of the study
328 focusing on a new non-stationary model development.

329 On the other hand, one could argue why not choose a geologically well-
330 investigated fault (e.g., the Chelungpu fault) in Taiwan as the model application to reduce
331 uncertainty, and here is our response: The “rock-mechanics” parameters of the model
332 (such as lateral pressure coefficients, variability of stress increment, and the strength
333 parameters of fault planes) are not clear either, even for those so-called well-investigated
334 faults in Taiwan. As a result, no matter which fault was selected as the model application,
335 engineering judgment must involve in the determinations of those “rock-mechanics”
336 parameters, more or less creating the same level of uncertainty when it comes to site
337 characterizations on stress increment variability, lateral earth pressure in rock, etc.

338 Besides, as mentioned previously the key reason of using the Meishan fault as a
339 case study is owing to its imminent earthquake risk, not to mention the well-characterized
340 return period of 162 years from the Central Geological Survey Taiwan (Lin et al., 2008)
341 could somewhat help increase the reliability of the estimate, in a comparison to other
342 cases without a well-characterized earthquake return period, or at least not yet reported.

343

344 5.2 Model improvements

R2.4

345 Certainly, the non-stationary analysis of the study can be further modified. For
346 example, in addition to the algorithms for thrust faults and strike-slip faults that have
347 been derived, the model is also applicable to normal faults as those Mohr circles shown in
348 Fig. 11. Accordingly, the minor principal stress at initial state ($\sigma_{3_initial}$) is equal to

349 $\gamma \times d \times K$ for this case, with the minor principal stress at time t^* (denoted as $\sigma_{3_{t^*}}$) that
350 can be expressed as $\sigma_{3_{initial}} - t^* \times ASI$. Next, the same probability calculation is
351 applicable by comparing the minor principal stress at t^* to the minor principal stress at
352 failure ($\sigma_{3_{failure}}$), for such a normal-fault earthquake subject to tectonic extension.

353 Further improvements can be conducted with the consideration of the direction of
354 stress increment, or the direction of tectonic compression/extension. Under the
355 circumstances, the Mohr circles of the initial state and failure state are shown in Fig. 12,
356 with major and minor principal stresses both varying with time.

357 Nevertheless, no matter how the non-stationary model will evolve, such type of
358 non-stationary analysis from the Mohr-Coulomb failure criterion is as novel, robust and
359 transparent as its counterparts, providing a new alternative to non-stationary earthquake
360 assessment related to a given active fault.

361

362 5.3. Earthquake should be stationary or non-stationary?

363 Although characteristic earthquakes related to a given active fault should be non-
364 stationary, in the 1970s a study has provided statistical evidence to the opposite:
365 earthquake is stationary (Gardner and Knopoff, 1974). However, it must be noted that
366 the study was not focusing on characteristic earthquakes, but based on the regional
367 seismicity in California.

368 Fig. 13 is a schematic diagram that helps explain the difference between the two
369 problems. For each fault, the recurring earthquake should be a non-stationary process,
370 and the non-stationary earthquake probability would be reset at the last event and
371 gradually increase with time. By contrast, the seismicity in a region would become

372 stationary with so many non-stationary processes present. For example, at $T = t_0$ (see Fig.
373 13), the sum of that many stationary probabilities should be close to that at $T = t_1$ (or at
374 any moment), although the earthquake probability induced by Fault D should be very low
375 at $T = t_0$, while others are higher.

376 The relationship can be simply explained with the patron-and-bank analogy. For
377 each patron (analogy to each fault), going to the bank is obviously a non-stationary
378 process, with the probability increasing with time since the very last visit. But for the
379 banks (analogy to the seismicity), it is a stationary process for them, as dealing with so
380 many patrons or so many non-stationary processes at one time.

381

382 **6. Summary and conclusion**

383 Given the earthquake recurrence associated with an active fault that should be a
384 non-stationary process, this paper introduces a new non-stationary analysis to evaluate
385 earthquake probability within a given period of time. Different from previous models,
386 the new analysis more clearly defines and calculates two earthquake stress states, on the
387 basis of the well-established, Mohr-Coulomb failure criterion.

388 In addition, this paper also presents a model application to evaluate earthquake
389 probability associated with the Meishan fault in central Taiwan. With the best-estimate
390 return period of 162 ± 50 years, focal depth of 4 ~ 8 km, etc., the active fault has a 7.6%
391 probability (standard deviation equal to 3.3%) of inducing the next Meishan earthquake
392 in 2015 ~ 2025, and if the earthquake does not recur by 2025, then the non-stationary
393 probability will increase to 8% in 2025 ~ 2035, rather than being unchanged, stationary,
394 or independent of the starting dates of a given period of time.

R2.6

395 **Notations**

R1.6

t_0	The time when the last event occurs
t^*	The time interval after the last event
$\sigma_{1_{t^*}}$	Major principle stress at time t^*
$\sigma_{1_{failure}}$	Major principle stress at failure state
$\sigma_{3_{failure}}$	Minor principal stress at failure state
c	Cohesion of the fault plane
ϕ	Friction angle of the fault plane
d	Earthquake focal depth
γ	Rock unit weight
K	Coefficient of lateral earth pressure in rock
ASI	Annual stress increment
\tilde{t}	Earthquake return period
$\sigma_{1_{\tilde{t}}}$	Major principal stress at return period
E	Expected value or mean value
V	Variance
μ_{ASI}	Mean value of ASI
n	Coefficient of variation for ASI
s_{ASI}	Standard deviation of ASI
$s_{\sigma_{1_{t^*}}}$	Standard deviation of $\sigma_{1_{t^*}}$
$\sigma_{1_{initial}}$	Major principal stress at initial state
$\sigma_{3_{initial}}$	Minor principal stress at initial state
$\sigma_{3_{t^*}}$	Minor principal stress at t^*

R2.6

396

397 **Acknowledgements**

398 We appreciate the comments on the submission from Editor Dr. Keefer, reviewer
 399 Dr. Chan of Nanyang Technological University and the anonymous reviewer, making it
 400 much improved in so many aspects after revision. We also appreciate the financial

R.2.2

Table 1. Summary of the model parameters used in the analyses

Parameters	Focal depth (km)	Unit Weight (kN / m ³)	Cohesion (MN / m ²)	Friction angle (degrees)	Return period (years)	K*	η^{**}
Range	4 ~ 8	25 ~ 30	3.6 ~ 22.7	22 ~ 46	112 ~ 212 (162 ± 50) 62 ~ 262 (162 ± 100)	0.2 ~ 0.5	0.25 ~ 1.0
Average	6	27.5	13.2	34	162	0.35	0.63

R 2.7

* K = the coefficient of lateral earth pressure in rock; ** η = the coefficient of variation for annual stress increment

R1.1

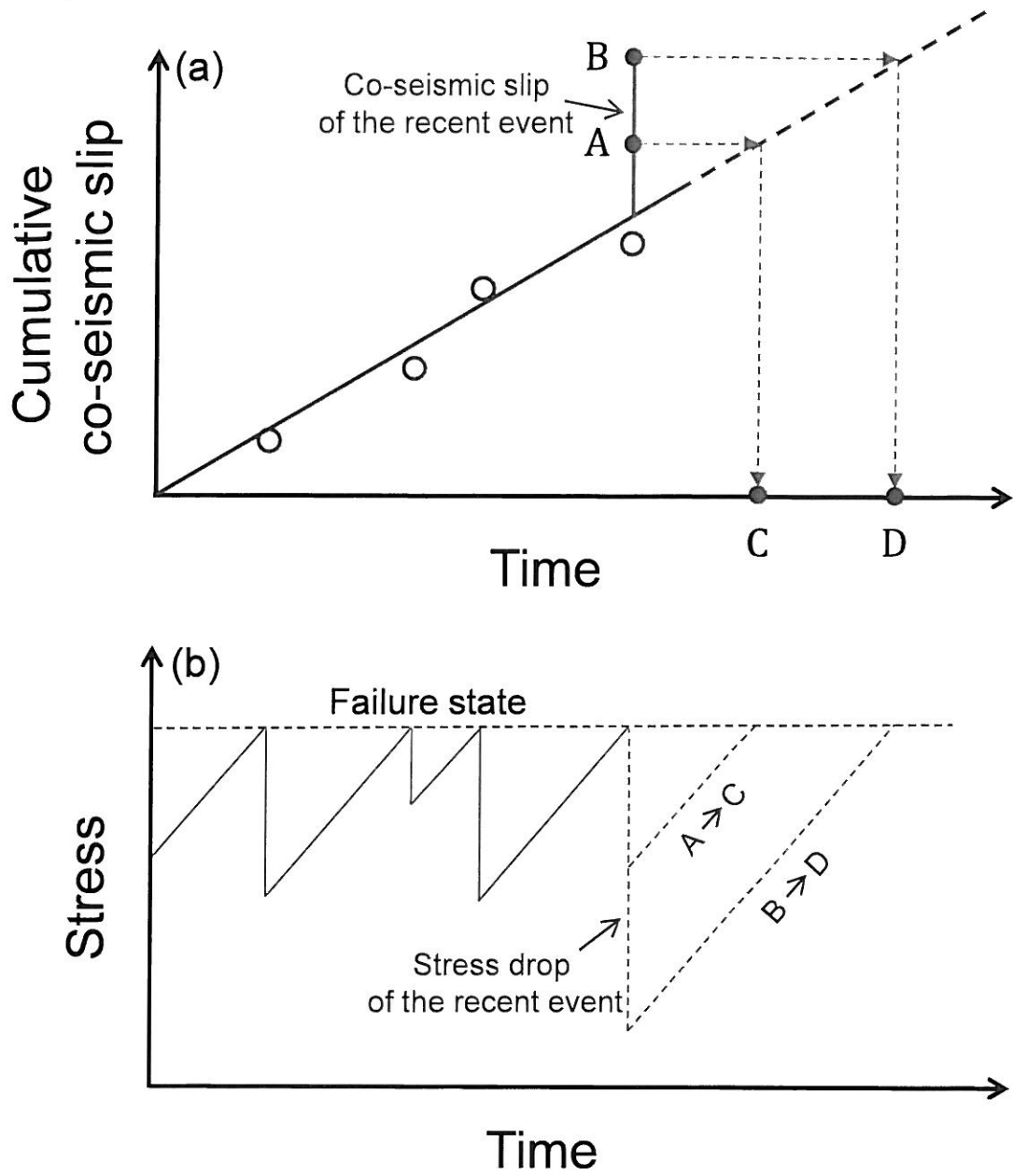


Fig. 1 Schematic diagram for the time-predictable model: a) best-estimate relationship between cumulative co-seismic slips and time, and b) the earthquake-time prediction facilitated with a failure state and a constant stress increment

R1.1

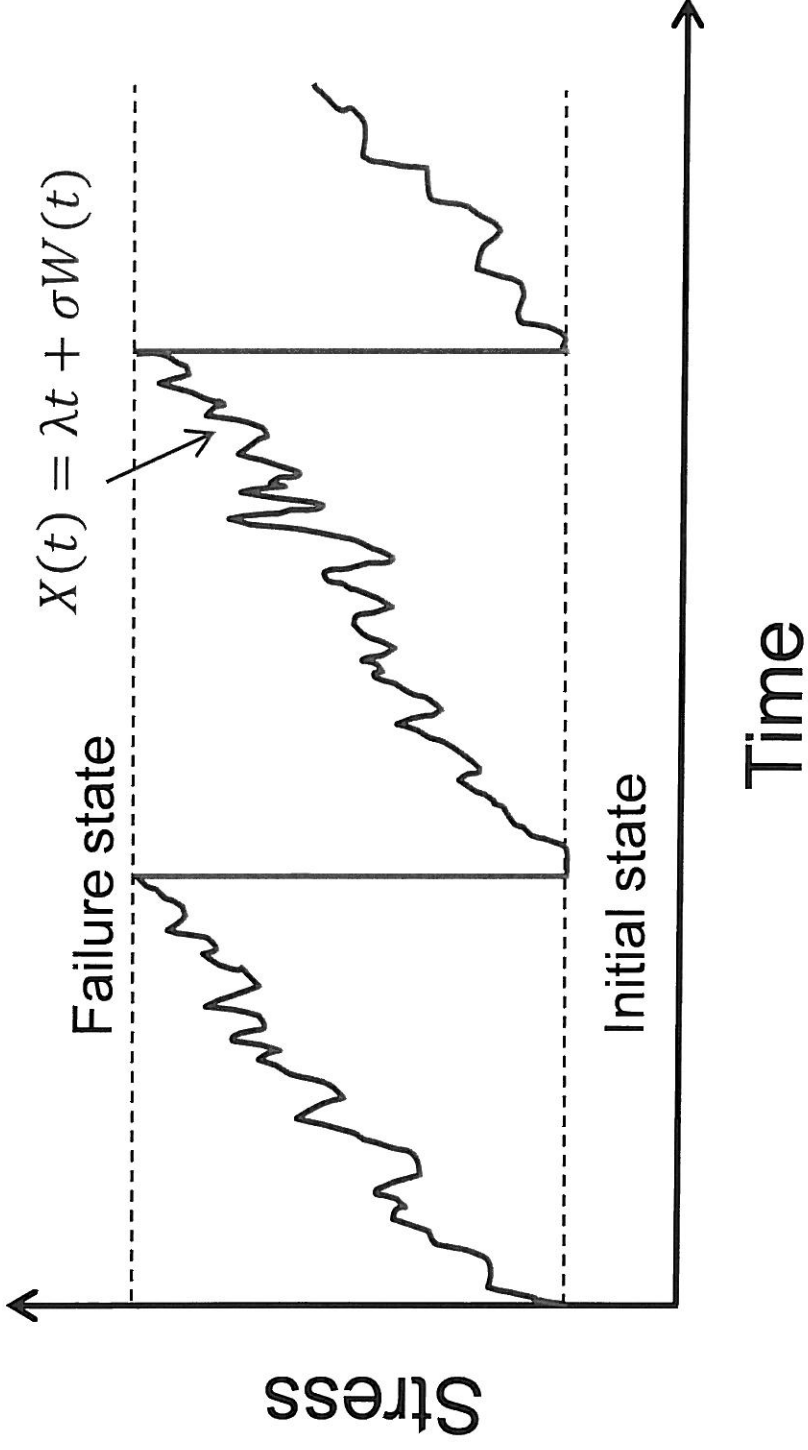


Fig. 2 Schematic diagram showing the essential of the Brownian model; within the two imaginary stress states, the model considers the stress-time series should be random and could be modeled by a long-term stress increment and a Brownian motion as $X(t) = \lambda t + \sigma W(t)$, where $X(t)$ is the stress at time t , λ is long-term stress increment rate, σ is the magnitude of a Brownian motion $W(t)$.

R1.1

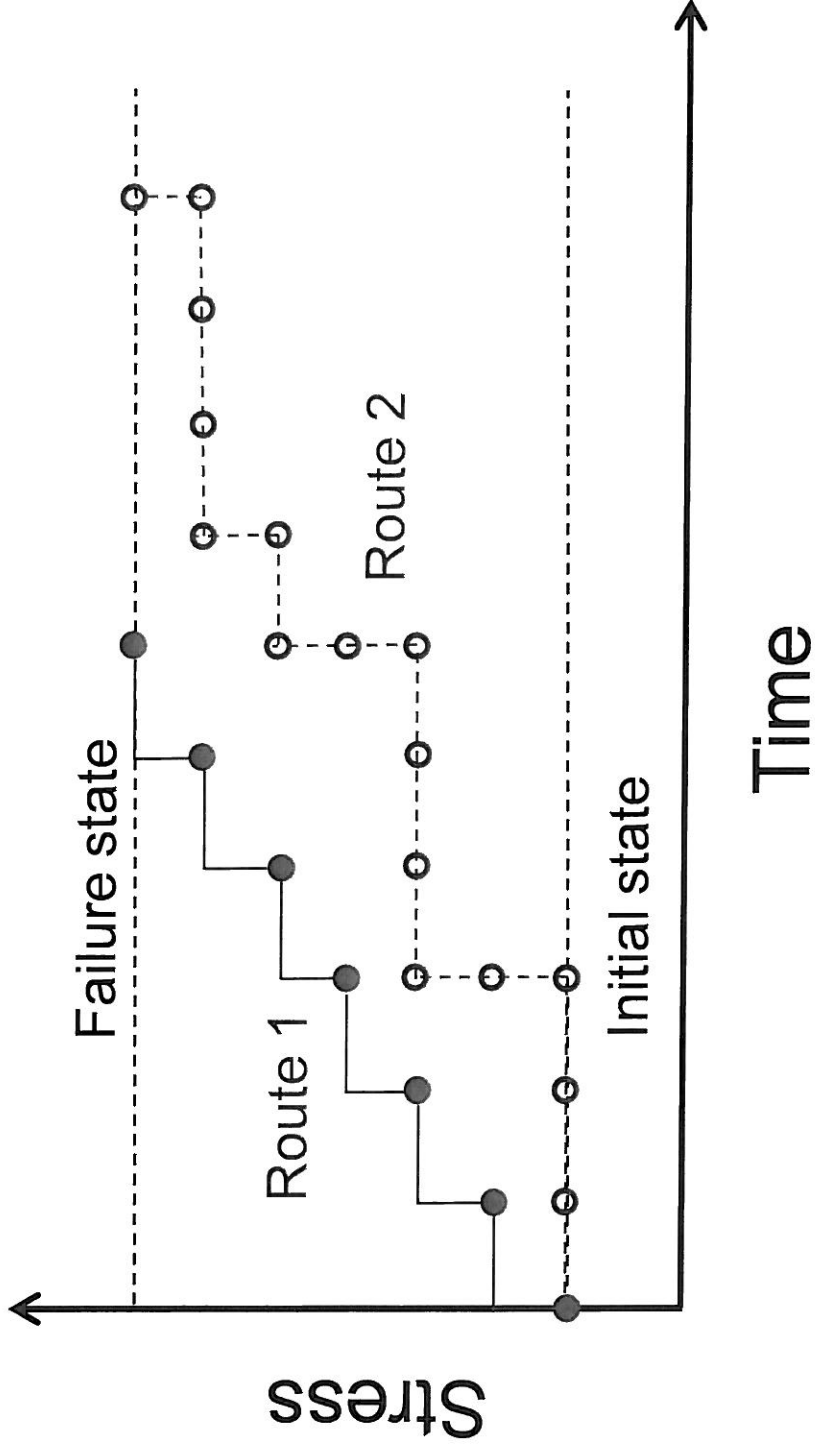


Fig. 3 Schematic diagram illustrating the negative binomial model; between the two stress states, many “stress routes” can be present, and the probability of each route can be estimated with the model, then developing the probability distribution for the interval between two consecutive events

R2.4

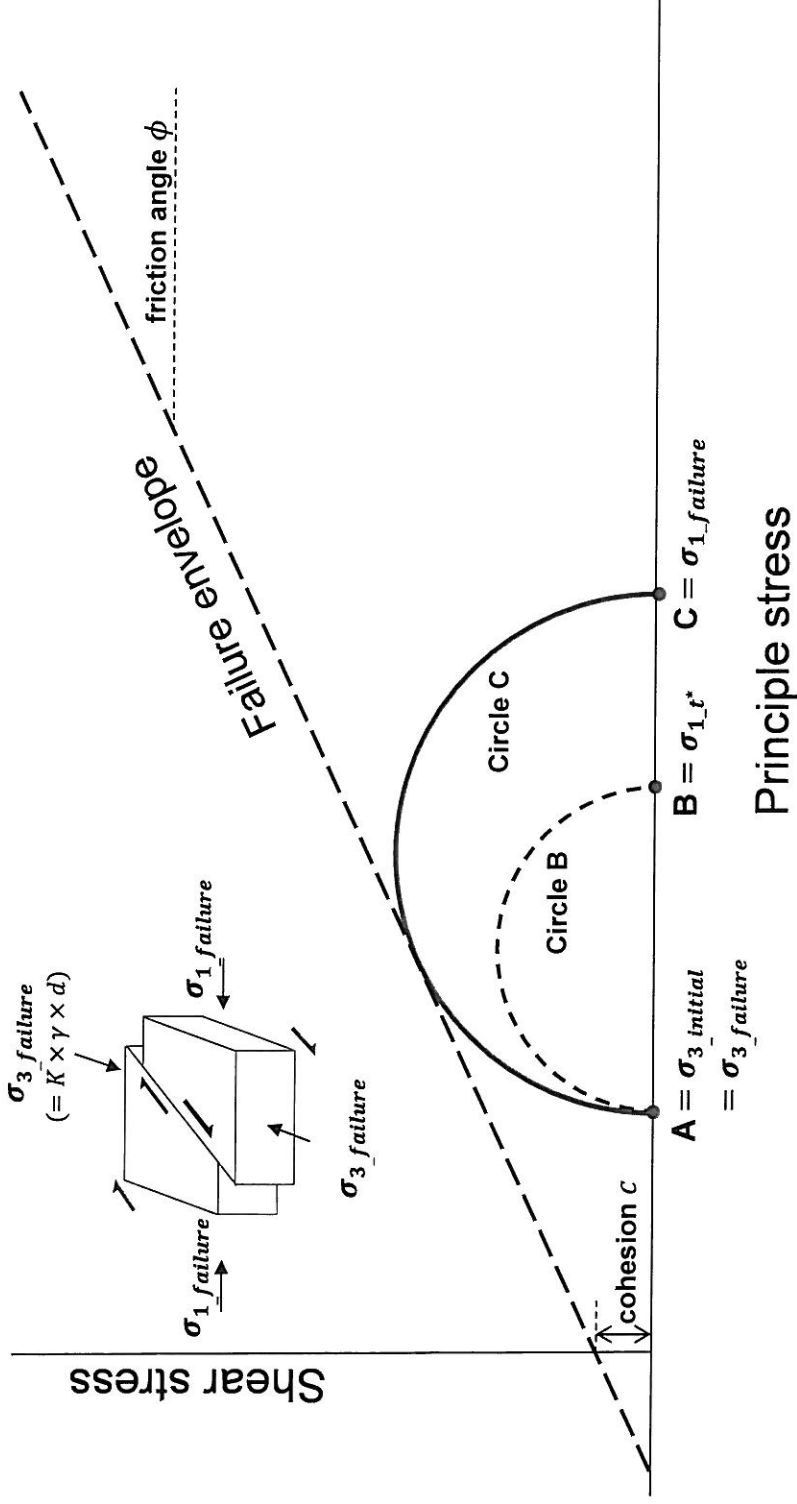


Fig. 5 The Mohr circles for evaluating the non-stationary earthquake probability for strike-slip earthquakes

R 1.4

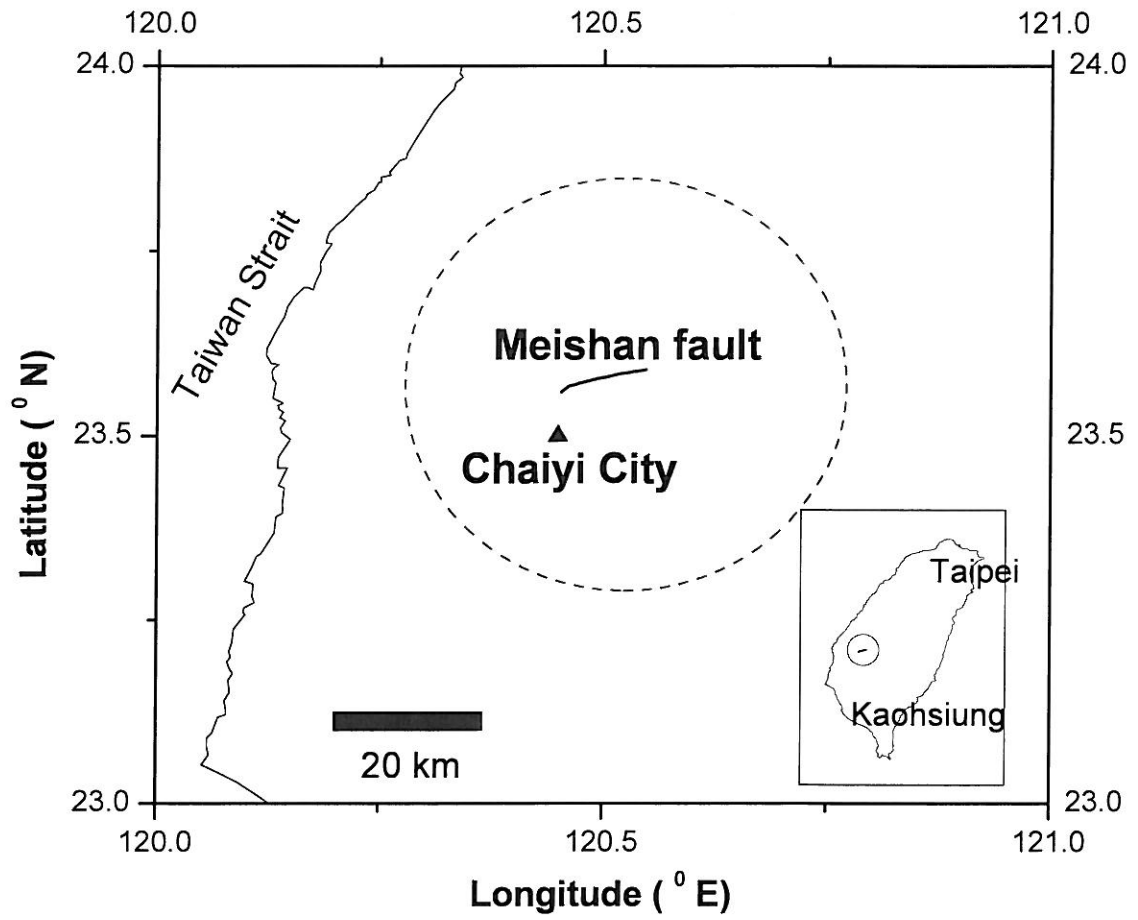


Fig. 7 The location of the Meishan fault in central Taiwan

R 2.4

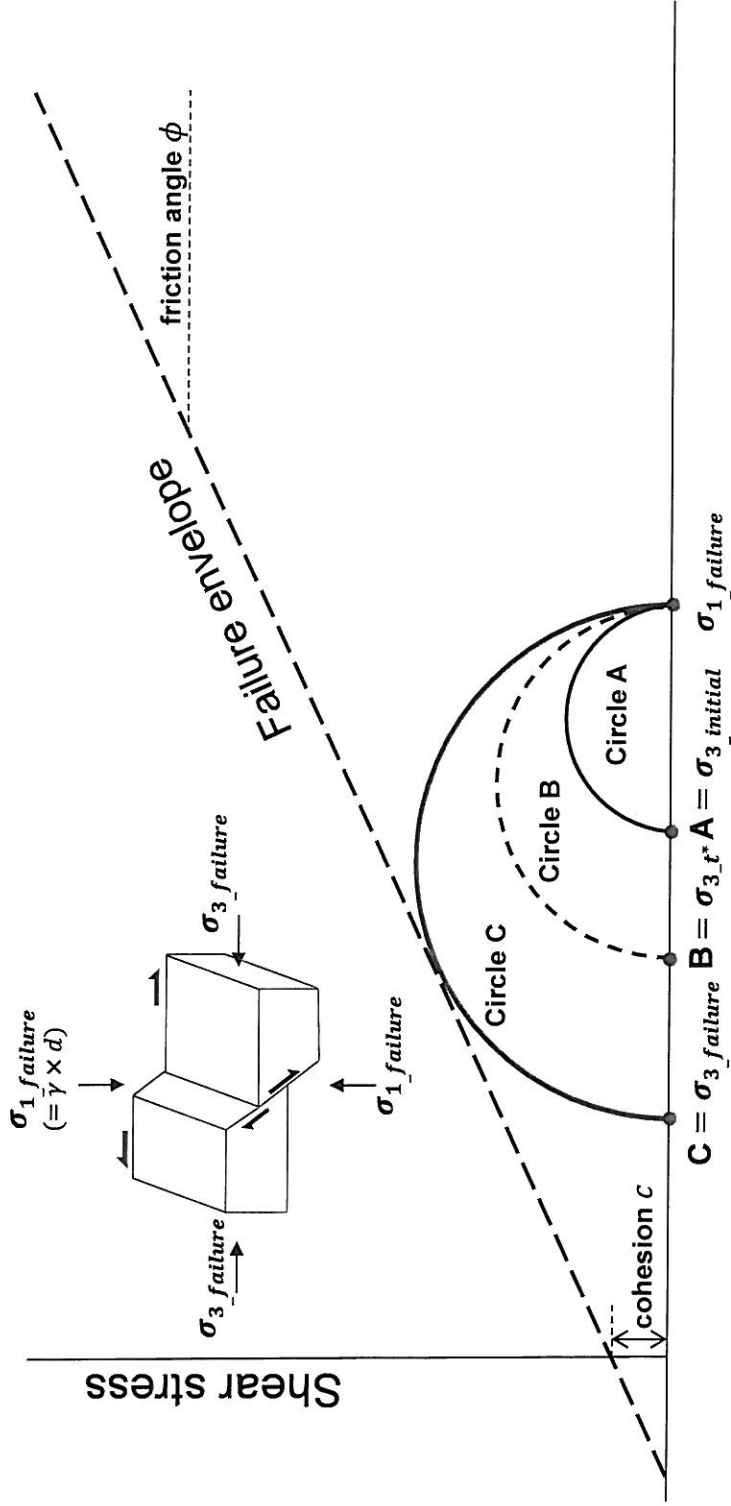


Fig. 11 The Mohr circles for evaluating the non-stationary earthquake probability for normal-fault earthquakes